

# Kernelized Edge Attention: Addressing Semantic Attention Blurring in Temporal Graph Neural Networks

Govind Waghmare<sup>1</sup>, Srinivas Rohan Gujalla Leel<sup>1</sup>, Nikhil Tumbde<sup>\*1</sup>,  
Sumedh B G<sup>\*1</sup>, Sonia Gupta<sup>1</sup>, Srikanta Bedathur<sup>2</sup>

<sup>1</sup>Mastercard, <sup>2</sup>Indian Institute of Technology, Delhi

{govind.waghmare, srinivasrohan.gujallaleel, nikhil.tumbde, sumedh.bg, sonia.gupta}@mastercard.com, srikanta@cse.iitd.ac.in

## Abstract

Temporal Graph Neural Networks (TGNNs) aim to capture the evolving structure and timing of interactions in dynamic graphs. Although many models incorporate time through encodings or architectural design, they often compute attention over entangled node and edge representations, failing to reflect their distinct temporal behaviors. Node embeddings evolve slowly as they aggregate long-term structural context, while edge features reflect transient, timestamped interactions (e.g. messages, trades, or transactions). This mismatch results in semantic attention blurring, where attention weights cannot distinguish between slowly drifting node states and rapidly changing, information-rich edge interactions. As a result, models struggle to capture fine-grained temporal dependencies and provide limited transparency into how temporal relevance is computed. This paper introduces KEAT (Kernelized Edge Attention for Temporal Graphs), a novel attention formulation that modulates edge features using a family of continuous-time kernels, including Laplacian, RBF, and learnable MLP variant. KEAT preserves the distinct roles of nodes and edges, and integrates seamlessly with both Transformer-style (e.g., DyGFormer) and message-passing (e.g., TGN) architectures. It achieves up to 18% MRR improvement over the recent DyGFormer and 7% over TGN on link prediction tasks, enabling more accurate, interpretable and temporally aware message passing in TGNNs.

## Code —

<https://waghmaregovind.github.io/KEAT-TemporalGNN>

## Introduction

Learning from time-evolving graph data is critical to applications such as recommendation, event forecasting, and fraud detection. While Graph Neural Networks (GNNs) have proven effective on static graphs (Kipf and Welling 2017; Hamilton, Ying, and Leskovec 2017; Liao et al. 2019), adapting them to continuous-time dynamics poses fundamental challenges (Kazemi et al. 2020; Longa et al. 2023; Zheng, Yi, and Wei 2025). TGNNs address this by modeling both structural and temporal dependencies, often through specialized architectures like temporal walks (Wang et al. 2021b), sequence patching (Yu et al. 2023), and alternative

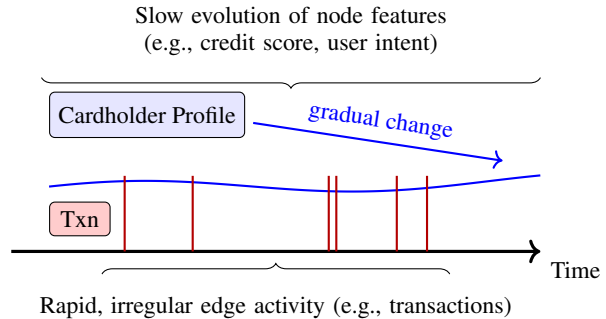


Figure 1: Temporal mismatch in dynamic graphs. While user profiles (nodes) change gradually (e.g., credit behavior), interactions like transactions (edges) vary rapidly and irregularly. Attention mechanisms in existing TGNNs often entangle these signals, leading to semantic attention blurring.

message-passing (Luo and Li 2022; Cong et al. 2023), or via time encodings (Chen et al. 2025; Xu et al. 2020, 2019).

To model temporal relationships in graph, attention-based TGNNs have gained popularity, particularly those inspired by Transformer architectures (Wu, Fang, and Liao 2024; Yu et al. 2023; Rossi et al. 2020). These models extend self-attention to graphs by assigning learnable importance scores to neighboring nodes and edges. While effective, most existing approaches compute attention over entangled node and edge representations. They fail to explicitly modulate edge features based on complex temporal dynamics, overlooking the fact that nodes and edges often evolve at different temporal rates. See Figure 1 for an illustration of this mismatch.

For instance, in financial transaction graphs, cardholder profiles (nodes) evolve gradually, reflecting changes like creditworthiness or spending behavior. Whereas, transaction records (edges) vary rapidly and irregularly, especially in the presence of suspicious or high-frequency activity. Capturing these short-term edge patterns without overwhelming them with slowly drifting node context is crucial for temporal precision. In particular, these models do not directly encode how time should modulate attention weights or influence message aggregation. This leads to *semantic attention blurring*, where slowly evolving node embeddings, capturing long-term structural context, are mixed indiscriminately

<sup>\*</sup>These authors contributed equally.

Copyright © 2026, Association for the Advancement of Artificial Intelligence (www.aaai.org). All rights reserved.

with sparse, transient edge features that carry rich, recent information. As a result, attention mechanisms struggle to prioritize temporally and semantically relevant interactions, reducing both temporal fidelity and interpretability.

While prior works focus on improving time encodings to address these issues, such efforts may offer limited returns under current attention formulations, such as those implemented in `TransformerConv`<sup>1</sup>, where attention scores are computed over the sum of node and edge projections. This formulation, or slight variations of it, is adopted in models such as TGN (Rossi et al. 2020), DyGFormer (Yu et al. 2023), and others (Xu et al. 2020), which similarly suffer from an inability to disentangle temporally distinct signals. As a result, such aggregation blurs temporal distinctions, making it difficult to separate recent, informative edge events from older or semantically unrelated interactions. This phenomenon is illustrated in Figure 2. In contrast, we shift the focus from time encoding design to the attention mechanism itself. By modulating only edge features, **comprising raw edge attributes and time encodings**, with continuous-time kernels, we introduce explicit temporal awareness into the attention computation and message aggregation. Crucially, our formulation is compatible with, and often enhances, existing time encoding schemes, making it broadly applicable and encoding-agnostic.

In this work, we propose a novel temporal attention formulation that directly addresses the mismatch in temporal dynamics between node and edge features in TGNNs. We call our framework **KEAT (Kernelized Edge Attention for Temporal Graphs)**. KEAT applies a family of continuous-time kernels exclusively to edge features, thereby incorporating temporal sensitivity into attention without altering node semantics. The key idea is simple yet effective: edge-time features are modulated via kernel functions such as Laplacian, RBF, or a learnable MLP-based variant. This modulation is applied within the key and value projections of attention, allowing recent interactions to be emphasized while preserving the relatively stable, slow-evolving role of node embeddings. KEAT integrates seamlessly with Transformer-style and message-passing TGNNs and remains agnostic to specific time encoding schemes.

Existing models like DyGFormer (Yu et al. 2023) leverage temporal patches and time-interval encodings to capture evolving graph dynamics. However, they still rely on conventional attention formulations and inherit similar limitations. We show that integrating KEAT into DyGFormer and other TGNN architectures improves temporal precision, interpretability, and predictive performance. These gains validate the broad applicability and plug-and-play nature of KEAT across diverse temporal modeling settings. Our key contributions are summarized as follows:

- We formally identify the issue of *semantic attention blurring* in Transformer-based TGNNs, where attention scores over combined node and edge projections hinder temporal precision and interpretability.

<sup>1</sup>Documentation for `TransformerConv`: [https://pytorch-geometric.readthedocs.io/en/stable/generated/torch\\_geometric.nn.conv.TransformerConv.html](https://pytorch-geometric.readthedocs.io/en/stable/generated/torch_geometric.nn.conv.TransformerConv.html) (Fey and Lenssen 2019)

- To resolve this, we introduce KEAT, a time-aware attention mechanism that applies continuous-time kernel modulation exclusively to edge features, preserving the distinct temporal roles of nodes and edges.
- KEAT is agnostic to time encoding schemes and compatible with a range of TGNN architectures. It requires minimal architectural changes and no additional supervision, making it practical for integration into existing systems.
- Through extensive experiments on dynamic graph benchmarks, we demonstrate that KEAT improves accuracy, enhances temporal fidelity, and produces interpretable attention patterns aligned with evolving edge dynamics.

## Related Work

**Temporal Graph Neural Networks.** TGNNs extend GNNs to dynamic graphs by modeling both structure and time. Early methods such as TGN (Rossi et al. 2020), TGAT (Xu et al. 2020), and CAWN (Wang et al. 2021b) incorporate time using continuous-time encodings or time-difference embeddings. Other approaches adopt positional or sinusoidal encodings inspired by language models (Xu et al. 2019). Recent work like LeTE (Chen et al. 2025) introduces a learnable transformation framework for time encoding using nonlinear mappings such as Fourier and splines, aiming to unify and generalize existing encoding schemes. Despite these advances, most of these models assume that better time encodings alone will yield better performance. In contrast, we argue that time encoding improvements have limited effect if the attention formulation itself cannot separate the dynamics of node and edge features. Our work departs from this direction by keeping time encodings fixed and focusing instead on making attention computations explicitly time-aware through kernel-based modulation.

**Attention Mechanisms in TGNNs.** Transformer-inspired TGNNs such as TGAT (Xu et al. 2020), TGN (Rossi et al. 2020), and DyGFormer (Yu et al. 2023) use attention to weigh the influence of temporal neighbors during message passing. These models often follow the `TransformerConv` formulation, a standardized implementation from the PyTorch Geometric, computing the attention scores from the sum of projected node and edge features. This design simplifies computation but introduces semantic attention blurring, wherein temporally distinct messages are mixed. Some methods attempt to refine attention using structural bias (e.g., CAWN’s walk-based decay (Wang et al. 2021b)), and a few incorporate time signals into attention projections through time encodings (Xu et al. 2020), but explicit time-aware modulation, such as continuous-time scaling of attention inputs, remains under-explored. Our kernel-based attention addresses this gap by decoupling edge dynamics from node semantics via time-dependent scaling, providing a lightweight yet effective way to inject temporal information into the attention mechanism.

**Modulated Attention Beyond TGNNs.** Time-aware attention has been studied in other domains such as NLP, time series and credit risk modeling. In language models, temporal self-attention augments Transformer-based architec-

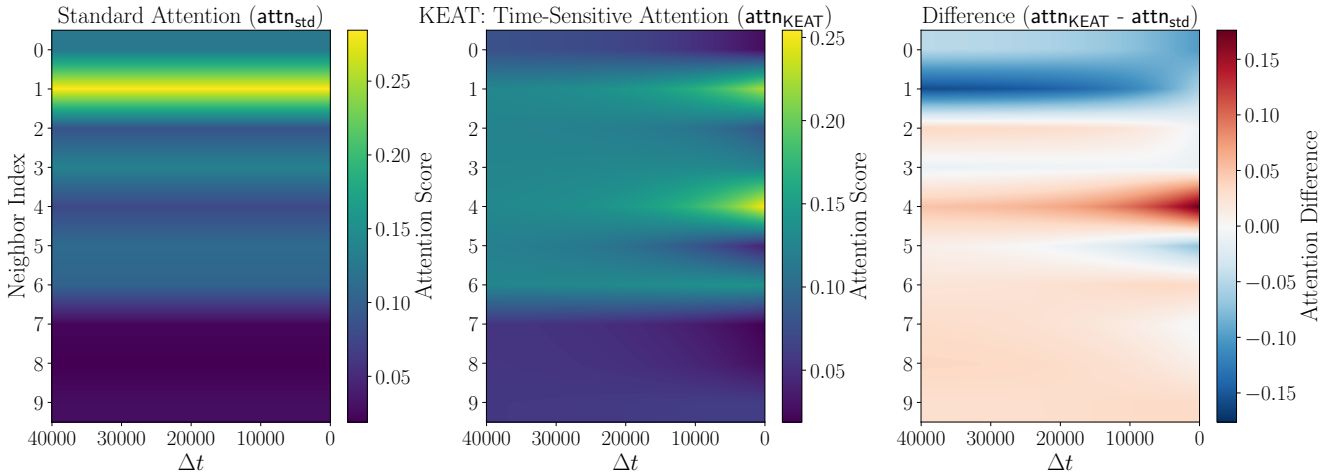


Figure 2: Temporal attention on `t.gbl-wiki` illustrating **semantic attention blurring**. We plot attention over ten neighbors across relative time  $\Delta t$ . (Left) Standard attention assigns uniform attention values across time for each neighbor, leading to semantic blurring. This shows invariance of attention to time encodings or  $\Delta t$ . (Middle) KEAT introduces time-aware modulation, emphasizing recent (smaller  $\Delta t$  value) and contextually relevant edges. (Right) The difference highlights how KEAT corrects the blurred focus of standard attention. See experimental section for details.

tures with timestamped text (Rosin and Radinsky 2022). Powerformer (Hegazy, Mahoney, and Erichson 2025) and (Niu et al. 2024) treat attention as the primary representation for time series. In credit risk assessment, DGNN-SR (Yuan et al. 2025) integrates multiple time perspectives directly into the attention module. In static graphs, Gradformer (Liu et al. 2024) applies exponential decay to graph transformer. Works like (Press, Smith, and Lewis 2022; Chi et al. 2022) study attention in NLP for extrapolation. While these works make attention more expressive, our approach introduces a modular, temporally kernel-based attention mechanism that applies time-conditioned scaling exclusively to edge representations, thus decoupling node and edge dynamics. This formulation allows time to play a more explicit role in the attention computation and helps reduce semantic attention blurring in a more interpretable way.

**Temporal Information Modeling.** Several TGNNs incorporate temporal information through auxiliary mechanisms rather than within attention. JODIE (Kumar, Zhang, and Leskovec 2019) applies time-conditioned projections to evolve user embeddings, and DyRep (Trivedi et al. 2019) models temporal interactions via point processes intensities. TGN (Rossi et al. 2020) maintains time-aware memory modules, while CAWN (Wang et al. 2021b) integrates temporal signals during neighbor sampling. In contrast, our approach embeds temporal characteristics directly into the attention computation by modulating edge features with kernel-weighted time encodings. This enables interpretable, differentiable, and architecture-agnostic modulation.

**Modular and Extendable TGNN Designs.** Recent architectures such as DyGFormer (Yu et al. 2023) adopt patch-based attention blocks to process temporally localized subgraphs. While these designs improve scalability and tem-

poral resolution, they still compute attention using mixed node-edge projections. Our kernel-based formulation can be seamlessly integrated into such architectures, enhancing their temporal fidelity without disrupting their tokenization, encoding, or aggregation pipelines. This highlights the flexibility of our method as a plug-and-play module for improving temporal sensitivity in a wide range of TGNNs.

## Methodology

### Problem Setting and Notation

Let  $\mathcal{G} = (\mathcal{V}, \mathcal{E}, T)$  be a dynamic graph, where  $\mathcal{V}$  is the set of nodes,  $\mathcal{E} \subseteq \mathcal{V} \times \mathcal{V}$  is the set of timestamped edges, and  $T$  is the set of event times. Each interaction is a tuple  $(i, j, \mathbf{e}_{ij}, t_{ij})$ , with  $i, j \in \mathcal{V}$ ,  $\mathbf{e}_{ij} \in \mathbb{R}^{d_e}$  representing raw edge features, and  $t_{ij} \in \mathbb{R}_+$  denoting the interaction time. TGNNs typically capture temporal context by computing the time difference  $\Delta t = t_i - t_{ij}$  between the current query time  $t_i$  and a past interaction time  $t_{ij}$ . This  $\Delta t$  is encoded using a time encoding function  $\phi : \mathbb{R}_+ \rightarrow \mathbb{R}^{d_t}$ , producing  $\phi(\Delta t)$ . The temporal and raw edge features are then concatenated to form:  $\bar{\mathbf{e}}_{ij} = [\mathbf{e}_{ij} \parallel \phi(\Delta t)] \in \mathbb{R}^{d_e + d_t}$ . Given the temporal neighborhood  $\mathcal{N}(i)$  of node  $i$ , the objective is to compute updated node embeddings  $\mathbf{h}'_i \in \mathbb{R}^d$  that are both structurally informative and temporally sensitive.

### Transformer-style Temporal Message Passing

Transformer-based attention mechanisms are widely adopted in TGNNs for aggregating messages from temporal neighbors. A representative implementation, `TransformerConv` (Fey and Lenssen 2019), computes attention from a source node  $i$  to a target node  $j$  as:

$$\alpha_{ij} = \text{softmax}_j \left( \frac{(\mathbf{W}_q \mathbf{h}_i)^\top (\mathbf{W}_k \mathbf{h}_j + \mathbf{W}_e \bar{\mathbf{e}}_{ij})}{\sqrt{d_k}} \right), \quad (1)$$

where  $\mathbf{h}_i, \mathbf{h}_j \in \mathbb{R}^d$  are node embeddings,  $\bar{\mathbf{e}}_{ij} \in \mathbb{R}^{d_e+d_t}$  is the concatenated edge-time feature, and  $\mathbf{W}_q, \mathbf{W}_k \in \mathbb{R}^{d' \times d}$ ,  $\mathbf{W}_e \in \mathbb{R}^{d' \times (d_e+d_t)}$  are learnable projection matrices. The attention is scaled by  $d_k = d'$  as in standard Transformers (Vaswani et al. 2017). The final embedding of node  $i$  is:

$$\mathbf{h}'_i = \mathbf{W}_{\text{self}} \mathbf{h}_i + \sum_{j \in \mathcal{N}(i)} \alpha_{ij} \cdot (\mathbf{W}_v \mathbf{h}_j + \mathbf{W}'_e \bar{\mathbf{e}}_{ij}), \quad (2)$$

where  $\mathbf{W}_v \in \mathbb{R}^{d' \times d}$ ,  $\mathbf{W}'_e \in \mathbb{R}^{d' \times (d_e+d_t)}$ , and  $\mathbf{W}_{\text{self}} \in \mathbb{R}^{d' \times d}$  are learnable weight matrices. This formulation, or variants of it, is used in several TGNNs such as TGN (Rossi et al. 2020), DyGFormer (Yu et al. 2023), and others.

## Time Encodings in Temporal Graphs

Popular time encoding functions  $\phi(\Delta t)$  include:

- **Fixed encodings:** GraphMixer (Cong et al. 2023) employs non-trainable sinusoidal time encodings, similar to the positional encodings used in standard Transformers.
- **Relative and learnable encodings:** TGN (Rossi et al. 2020) uses learnable sinusoidal embeddings for relative time, similar to TGAT (Xu et al. 2020), applied in both message computation and memory updates. LeTE (Chen et al. 2025) learns flexible time encoding functions using splines and Fourier-based transformations.

**Limitations of Time Encodings.** Time encodings  $\phi(\Delta t)$  in TGNNs are often concatenated with node or edge features (see Eq. 1 and 2) but do not explicitly influence the attention weights. As a result, they weakly capture temporal patterns like frequency or semantic relevance (Figure 2), limiting the model’s ability to differentiate diverse temporal interactions.

A common approach is to encode time differences  $\Delta t$  using sinusoidal functions such as  $\phi(\Delta t) = \cos(\omega \Delta t)$  or  $\sin(\omega \Delta t)$ . As shown in Appendix B, these simple periodic encodings capture only a limited subset of the moment spectrum of the inter-arrival distribution  $p(\Delta t)$ :

$$\mathbb{E}_{\Delta t}[\cos(\omega \Delta t)] = \sum_{n=0}^{\infty} \frac{(-1)^n \omega^{2n}}{(2n)!} \mathbb{E}[(\Delta t)^{2n}]. \quad (3)$$

While some prior works use both sine and cosine terms to capture more statistical moments (Chen et al. 2025), these encodings remain passive and fail to directly shape attention weights. As a result, they often miss temporal asymmetries important for aggregation. This limitation is exacerbated in real-world temporal graphs, where the distribution  $p(\Delta t)$  often shifts across training and validation sets (refer Appendix C). In many graphs, early interactions are typically sparse, while later ones are denser, causing skewed distributions and shifts in both the mean and higher-order moments.

KEAT addresses this challenge by introducing kernel-modulated encodings of the form  $f(\Delta t) = \psi(\Delta t) \cdot \bar{\mathbf{e}}_{ij}$ , where  $\psi(\Delta t)$  is a temporal kernel. This formulation expands into a full polynomial over  $\Delta t$  and becomes sensitive to all moments of  $p(\Delta t)$  (see Appendix B.2). Importantly, the modulated signal  $f(\Delta t)$  is used to directly influence attention computation, ensuring that time information shapes both the neighbor weighting and the final embedding output.

## Design Criteria for Temporal Kernels

To enable time-aware attention, we modulate edge features using a continuous temporal kernel  $\psi(\Delta t)$  that scales contributions based on the elapsed time  $\Delta t$ . The kernel should satisfy several desirable properties: (i) it should decay monotonically with increasing  $\Delta t$  to prioritize recent events; (ii) it must be bounded within  $[0, 1]$  to ensure numerical stability; (iii) it should be continuous to support smooth optimization; and (iv) it should be flexible. Parameterized MLPs can model richer, potentially non-monotonic (vs. Laplacian and RBF) temporal patterns when interpretability is less critical.

## Family of Temporal Kernels

We instantiate the temporal modulation function  $\psi(\Delta t)$  using the following kernel families:

- **Laplacian kernel:**  $\psi(\Delta t) = \exp\left(-\frac{\Delta t}{\sigma}\right)$
- **RBF kernel:**  $\psi(\Delta t) = \exp\left(-\frac{\Delta t^2}{\sigma^2}\right)$
- **Learned kernel (MLP):**  $\psi(\Delta t) = \text{MLP}(\Delta t)$

Here,  $\sigma$  denotes the standard deviation of inter-event time differences computed from the training set. The Laplacian and RBF kernels are parameter-free and introduce interpretable temporal biases by smoothly attenuating the influence of older interactions. In contrast, the MLP-based kernel offers greater flexibility, enabling the model to learn complex, data-driven modulation patterns. All variants are differentiable and integrate seamlessly into end-to-end training.

## Method: KEAT – Kernelized Attention over Time

We introduce KEAT, a mechanism that integrates temporal modulation into attention by applying a kernel  $\psi(\Delta t)$  to the edge-time feature  $\bar{\mathbf{e}}_{ij}$  before it influences attention or embedding updates. In Transformer-style architectures (Eq. 1) attention scores are computed from projected node embeddings and edge features. Node embeddings evolve slowly and capture long-term structural information, while edge features encode temporally localized, interaction-specific signals. Thus, modulating the edge component using a continuous-time kernel  $\psi(\Delta t)$  provides a principled way to inject temporal sensitivity. KEAT requires only a lightweight modification to edge projections, introducing negligible overhead during training or inference.

KEAT explicitly biases or modulates the attention toward different temporal interactions by scaling edge-time features via  $\psi(\Delta t)$ . The modified attention score becomes:

$$\alpha_{ij} = \text{softmax}_j \left( \frac{(\mathbf{W}_q \mathbf{h}_i)^\top (\mathbf{W}_k \mathbf{h}_j + \mathbf{W}_e [f(\Delta t)])}{\sqrt{d_k}} \right), \quad (4)$$

where,  $f(\Delta t) = \psi(\Delta t) \cdot \bar{\mathbf{e}}_{ij}$  and the corresponding node embedding update formula is:

$$\mathbf{h}'_i = \mathbf{W}_{\text{self}} \mathbf{h}_i + \sum_{j \in \mathcal{N}(i)} \alpha_{ij} \cdot (\mathbf{W}_v \mathbf{h}_j + \mathbf{W}'_e [f(\Delta t)]) \quad (5)$$

This design ensures that temporally closer interactions contribute significantly to attention computation and feature aggregation, while preserving the original Transformer architecture. Notably, node features remain unaltered, allowing a clean decoupling of structural and temporal contributions.

In DyGFormer (Yu et al. 2023), interaction histories are divided into patches, each summarizing a local neighborhood around source or destination nodes. To integrate KEAT, we modulate only the edge features within each patch using a representative patch timestamp (e.g., mean edge time). Specifically, the query is scaled by  $\exp(t_{\text{patch}})$  and the key by  $\exp(-t_{\text{patch}})$ , resulting in attention scores of the form  $\exp(t_{\text{query}} - t_{\text{key}})$ . This introduces a directional temporal bias, enabling time-sensitive attention without altering DyGFormer’s architecture. See Appendix D for details.

## Advantages of Kernel-Based Attention

KEAT offers several desirable properties: • **Temporal precision**: (Laplacian and RBF kernels) emphasizes recent interactions by downweighting distant ones; • **Semantic disentanglement**: isolates evolving edge patterns while preserving node semantics; • **Architectural generality**: seamlessly integrates into diverse TGNNs (e.g., TGN, TGAT, DyGFormer); • **Simplicity and efficiency**: lightweight, differentiable, and requires no additional preprocessing.

Beyond demonstrating empirical utility, we provide theoretical justification for using temporal kernels in attention. In particular, we show that kernel-based modulation suppresses contributions from higher-order moments of the time distribution, improving robustness to distribution shifts across training and inference. The following theorem formally captures this effect for the Laplacian or RBF kernel  $\psi(t)$ :

**Theorem 1** *Let  $p(t)$  be a probability density function supported on  $[0, \infty)$  such that  $\mathbb{E}[t^n] < \infty$  and  $\mathbb{E}[\psi(t)t^n] < \infty$  for all  $n \geq 0$ , where  $\psi(t)$  is a non-negative, monotonically decreasing kernel function. Let  $\phi(t) = \sum_{n=0}^{\infty} c_n t^n$  be an analytic time encoding function with coefficients  $\{c_n\}$ . Define the kernel-to-base ratio for each moment order  $n$  as:*

$$R_n = \frac{\mathbb{E}[\psi(t)t^n]}{\mathbb{E}[t^n]}, \quad \text{with } R_0 = \mathbb{E}[\psi(t)].$$

*Then, the sequence  $\{R_n\}_{n=0}^{\infty}$  is strictly decreasing and converges to zero:  $\lim_{n \rightarrow \infty} R_n = 0$ . As a result, the expected kernel-weighted time encoding  $\mathbb{E}[\psi(t) \cdot \phi(t)]$  becomes increasingly dominated by lower-order terms<sup>2</sup>.*

The proof is provided in Appendix E. In addition, we establish a complementary result: incorporating temporal kernels into attention reduces the variance of the attention logits. This promotes more stable neighbor weighting, particularly under temporally imbalanced or skewed interaction histories. This variance-reduction effect further underscores the robustness and interpretability benefits of kernel-based attention. See Appendix E for a complete derivation.

## Experiments

We empirically validate the effectiveness of our proposed temporal kernel modulation framework across multiple dynamic graph learning tasks. Our evaluation focuses on three key aspects: (1) compatibility and integration with existing

<sup>2</sup>This formulation naturally extends to expectations of the form  $\mathbb{E}[\psi(t) \cdot \mathbf{e}_{ij}]$ , as used in Equations 4 and 5.

attention-based TGNN architectures, (2) the ability to capture fine-grained temporal dependencies through moment-aware attention modulation, and (3) performance gains under varying temporal encodings and graph dynamics.

Experiments are primarily conducted on the Temporal Graph Benchmark (TGB) (Huang et al. 2023), which provides large-scale, realistic datasets with diverse temporal characteristics. To further evaluate the generality and robustness of our kernelized attention mechanism, we extend the benchmark suite by incorporating additional datasets from the JODIE (Kumar, Zhang, and Leskovec 2019) framework for dynamic link prediction, as well as the DGraphFin dataset (Huang et al. 2022) for dynamic node classification. This extended evaluation suite enables us to test KEAT across a wider range of temporal graph settings, including financial graphs, and user-item interactions.

KEAT is implemented as a lightweight, modular enhancement to existing Transformer-based TGNNs without requiring architectural changes. We report results using standardized splits and evaluation metrics to isolate the impact of temporal attention modulation. Unless stated otherwise, we use the Laplacian kernel by default. A detailed description of datasets along with statistics is provided in Appendix C.

## Task Definitions

We consider two standard tasks on temporal graphs  $\mathcal{G}$ . In **dynamic link prediction**, the objective is to estimate the probability of a link between two nodes at a given time, framed as a ranking problem with Mean Reciprocal Rank (MRR) as the metric. For JODIE datasets, we measure performance using AUC and Average Precision (AP). In **dynamic node classification**, the goal is to predict a node’s label at a specific time based on its interaction history and temporal context, capturing evolving patterns such as user preferences or risk. Performance is evaluated using NDCG@10 for tgbn datasets and using AUC for the DGraphFin dataset.

**Baselines** Our proposed kernel-based attention mechanism is designed to enhance Transformer-style TGNNs. To evaluate its impact, we integrate it into two widely used attention-based architectures, TGN and DyGFormer, serving as our primary backbones. The resulting models, KEAT-TGN and KEAT-DyGFormer, are compared against their vanilla counterparts to isolate the effect of our contribution. We also report results from several strong baselines, including DyRep (Trivedi et al. 2019), TNCN (Zhang et al. 2024), and CTAN (Gravina et al. 2024), as well as memory-based methods EdgeBank<sub>tw</sub> and EdgeBank<sub>∞</sub> (Poursafaei et al. 2022), included in the TGB leaderboard. While some of these baselines do not explicitly model temporal attention, they provide valuable context for evaluating our method. Other baselines, such as TCL (Wang et al. 2021a), NAT (Luo and Li 2022), CAWN (Wang et al. 2021b), and Graph-Mixer (Cong et al. 2023) underperform compared to DyGFormer and/or TGB and are evaluated on a narrower set of datasets, as shown in the TGB leaderboard<sup>3</sup>. Appendix F summarizes baseline selection criteria, ranking on the link prediction task, their scalability and dataset coverage.

<sup>3</sup>[https://tgb.complexdatalab.com/docs/leader\\_linkprop/](https://tgb.complexdatalab.com/docs/leader_linkprop/)

Method	Split	tgb1-wiki	tgb1-review	tgb1-coin	tgb1-comment
EdgeBank <sub>tw</sub>	Val	0.600	0.024	0.492	0.124
	Test	0.571	0.025	0.580	0.149
EdgeBank <sub>∞</sub>	Val	0.527	0.023	0.315	0.109
	Test	0.495	0.023	0.359	0.129
DyRep	Val	0.072 ± 0.009	0.216 ± 0.031	0.512 ± 0.014	0.291 ± 0.028
	Test	0.050 ± 0.017	0.220 ± 0.030	0.452 ± 0.046	0.289 ± 0.033
TNCN	Val	0.741 ± 0.001	0.325 ± 0.003	0.740 ± 0.002	0.643 ± 0.003
	Test	0.718 ± 0.001	0.377 ± 0.010	0.762 ± 0.004	0.697 ± 0.006
CTAN	Val	—	—	—	—
	Test	0.668 ± 0.007	0.405 ± 0.004	0.748 ± 0.004	0.671 ± 0.067
TGN	Val	0.435 ± 0.069	0.313 ± 0.012	0.607 ± 0.014	0.356 ± 0.019
	Test	0.396 ± 0.060	0.349 ± 0.020	0.586 ± 0.037	0.379 ± 0.021
KEAT-TGN	Val	0.515 ± 0.053	0.324 ± 0.004	0.624 ± 0.012	0.368 ± 0.019
	Test	0.474 ± 0.031	0.380 ± 0.007	0.632 ± 0.023	0.400 ± 0.020
Improvement	Test	+7.76%	+3.10%	+4.62%	+2.10%
DyGFormer	Val	0.816 ± 0.005	0.219 ± 0.017	0.730 ± 0.002	0.613 ± 0.003
	Test	0.798 ± 0.004	0.224 ± 0.015	0.752 ± 0.004	0.670 ± 0.001
KEAT-DyGFormer	Val	0.829 ± 0.003	0.335 ± 0.020	—	—
	Test	0.815 ± 0.005	0.412 ± 0.012	0.803 ± 0.003	0.776 ± 0.001
Improvement	Test	+1.69%	+18.80%	+5.10%	+10.60%

Table 1: Link prediction results (MRR) on the TGBL benchmark datasets. We report both validation and test MRR for each method. All baseline results are taken from TGB leaderboard (Huang et al. 2023). **KEAT** denotes our kernel-based attention mechanism integrated into TGN and DyGFormer backbones. The top three test results for each dataset are highlighted using green (first), yellow (second), and gray (third). Entries marked with — indicate that baseline results are not available.

**Implementation Details.** We implement our model using PyTorch and PyTorch Geometric, and the official TGB framework (Huang et al. 2023). All experiments follow the default hyperparameters provided by the TGB benchmark to ensure fair and reproducible comparisons. Each experiment is run five times with different random seeds. The experimentation settings and hyperparameters for JODIE datasets and DGraphFin are provided in Appendix G.

**Link Prediction Results.** Table 1 presents the MRR for link prediction on the tgb1 benchmark datasets. Our method, Kernel-based Attention (KEAT), is applied to two popular TGNN backbones: TGN and DyGFormer. Across all datasets, KEAT variants demonstrate consistent improvements over their respective base models. Notably, KEAT-DyGFormer achieves the best test performance on all four datasets, tgb1-wiki, tgb1-review, tgb1-coin, and tgb1-comment, demonstrating the generality and effectiveness of our kernelized attention mechanism. KEAT-TGN also shows gains over TGN on all datasets, with improvements ranging from +2.1% to +7.8% in test MRR. These results affirm that augmenting TGNNs with time-sensitive, structure-aware attention yields measurable and consistent performance benefits. KEAT also demonstrates consistently stronger performance on the JODIE datasets across multiple evaluation metrics, highlighting its effectiveness in handling time-evolving interactions. Details are in Appendix G.

**Effect of Kernel Choice.** We evaluate the effect of different kernel choices within the KEAT framework through an ablation study using three variants: *Laplacian*, *RBF*, *MLP*, with a baseline (no kernel modulation). All experiments are conducted using the TGN backbone on three benchmark datasets, tgb1-wiki, tgb1-review, and tgb1-coin (see Table 2). The results consistently indicate that temporal kernels enhance performance. For instance, on tgb1-wiki, the Laplacian kernel yields an MRR of 0.474±0.031, marking a significant improvement of +7.8% over the no-kernel baseline (0.396±0.060). Similarly, the *RBF kernel* achieves the highest MRR on tgb1-coin at 0.636±0.021, surpassing the baseline by +5.0%. These gains underscore the benefit of temporally modulating edge features when computing attention.

Laplacian and RBF perform most consistently, benefiting from positive-definite, distance-based temporal modulation. MLP is more expressive but has higher variance, as it lacks built-in inductive bias and depends heavily on available data. Overall, these results highlight the generalization advantage of structured kernels in time-sensitive tasks.

**Choosing the Right Kernel.** Laplacian prioritizes recency, ideal for short-term temporal dynamics. In contrast, the RBF kernel provides a smoother, more balanced decay that captures both recent and mid-range dependencies. MLP is suited for high-data regimes with complex, non-

Method	Kernel	tgb1-wiki		tgb1-review		tgb1-coin	
		Val	Test	Val	Test	Val	Test
KEAT-TGN	Laplacian	0.515 $\pm$ 0.053	<b>0.474</b> $\pm$ 0.031	<b>0.324</b> $\pm$ 0.004	<b>0.378</b> $\pm$ 0.007	<b>0.624</b> $\pm$ 0.012	0.632 $\pm$ 0.023
	RBF	0.512 $\pm$ 0.027	0.437 $\pm$ 0.035	0.322 $\pm$ 0.008	0.374 $\pm$ 0.011	0.623 $\pm$ 0.015	<b>0.636</b> $\pm$ 0.021
	MLP	<b>0.524</b> $\pm$ 0.017	0.456 $\pm$ 0.027	<b>0.324</b> $\pm$ 0.007	0.372 $\pm$ 0.008	0.620 $\pm$ 0.022	0.617 $\pm$ 0.024
TGN	w/o Kernel	0.435 $\pm$ 0.069	0.396 $\pm$ 0.060	0.313 $\pm$ 0.012	0.349 $\pm$ 0.020	0.607 $\pm$ 0.014	0.586 $\pm$ 0.037

Table 2: MRR results on three TGBL datasets using different kernel types. Each cell reports mean  $\pm$  standard deviation for validation and test sets. Best results in each column (based on mean) are shown in bold.

monotonic temporal patterns but may underperform when supervision is limited. Overall, Laplacian and RBF offer strong, low-variance performance across settings. Unless otherwise specified, we use Laplacian as the default kernel.

**Node Classification Results.** KEAT consistently improves node classification performance when integrated into TGN across diverse tgbn datasets (refer Appendix G). On tgbn-trade and tgbn-genre, KEAT-TGN achieves substantial gains of +5.30% and +5.29% in test NDCG@10, respectively. These improvements highlight KEAT’s ability to inject temporal structure into attention mechanism, aligning node representations more closely with their evolving interaction context. Even on challenging datasets like tgbn-token, KEAT improves performance by +1.1%, indicating robustness. The slight but consistent gain on tgbn-reddit suggests that KEAT complements existing signals without degrading strong baselines. These findings reinforce KEAT’s effectiveness in stabilizing node-level predictions and improving temporal generalization. Refer Appendix G for results on DGraphFin.

**Impact of KEAT Across Time Encoding Strategies.** We evaluate the robustness of KEAT with various time encoding methods, including GraphMixer (non-learnable), TGN/TGAT(learnable), and LeTE(learnable, Fourier and Spline-based), on three datasets. Results in Appendix G (on tgb1-wiki, tgb1-review and tgb1-coin) demonstrate that KEAT consistently improves test MRR, regardless of the encoding strategy. For instance, on tgb1-wiki, KEAT improves test MRR by +7.8% with TGN/TGAT and +7.3% with LeTE. Even when the raw encodings are strong (e.g., GraphMixer on tgb1-review), KEAT improves or maintains performance. Importantly, we observe reduced variance across runs when KEAT is used, suggesting it helps regularize attention with structured inductive bias. These results indicate that KEAT is orthogonal to the choice of time encoding and acts as a plug-and-play enhancement for diverse temporal message-passing models.

Attention plots in Appendix G highlights how KEAT enables edge-modulated, time-sensitive attention over neighbors. Unlike standard attention, which yields flat, temporally agnostic weights, KEAT dynamically adjusts attention based on both edge timing and feature context. This allows attention to vary meaningfully with  $\Delta t$ , yielding sharper, context-aware focus that mitigates semantic attention blurring and enhances temporal discrimination. Furthermore, attention weight heatmaps over time (refer to Appendix G) il-

lustrate the interpretability of KEAT: they reveal how attention shifts gradually as edge timestamps grow older, offering insights into how the model prioritizes recent and semantically relevant interactions.

**Computational Complexity.** With Laplacian or RBF kernels, KEAT incurs no additional computational overhead and retains the same time and space complexity as its underlying backbone architectures, TGN and DyGFormer. MLP kernel operates on scalar time gaps with a few parameters. Under standard TGBL settings, we observe similar inference complexity of MLP kernel compared to other kernels.

**Extended results.** For completeness, we provide detailed dataset statistics, extended ablations (e.g., node vs. edge modulation, kernel width sensitivity), results on additional datasets (including JODIE and DGraphFin), full experimental settings, and theoretical proofs in Appendix. We encourage readers to refer to these sections for further insights. Together, these empirical results establish KEAT as a general-purpose enhancement for TGNNs. By embedding temporal structure directly into the attention computation, KEAT improves both predictive performance and training stability across datasets, time encoding schemes, and kernel types.

**Limitations of KEAT.** While KEAT demonstrates strong performance across datasets, it may be less effective in scenarios when edge activity is extremely sparse or highly clustered in time, which can limit the informativeness of temporal modulation. Addressing such challenging regimes remains an important and promising direction for future work.

## Conclusion

We presented KEAT, a kernel-based attention framework that addresses semantic attention blurring in TGNNs. By introducing temporal kernels into the attention mechanism, KEAT preserves fine-grained distinctions between recent and older edge interactions, enabling more precise temporal reasoning. The method is lightweight, model-agnostic, and compatible with diverse time encoding strategies. Empirical results on diverse datasets show consistent performance gains across multiple tasks and model backbones such as TGN and DyGFormer. Extensive ablations further confirm the impact of kernel choice, edge-level modulation, and reduced attention variance. Overall, KEAT offers a simple yet effective solution to improve both the accuracy and generalization of TGNNs with minimal overhead.

## Acknowledgments

Srikanta Bedathur acknowledges his DS Chair Professor of AI fellowship and the funding support from Mastercard AI Garage for this work.

## References

- Chen, X.; Tang, Y.; Xu, J.; Zhang, J.; Zhang, S.; Peng, S.; Zheng, X.; and Xiong, Y. 2025. Rethinking Time Encoding via Learnable Transformation Functions. In *International Conference on Machine Learning*.
- Chi, T.-C.; Fan, T.-H.; Ramadge, P. J.; and Rudnick, A. I. 2022. KERPLE: Kernelized Relative Positional Embedding for Length Extrapolation. In *International Conference on Neural Information Processing Systems*.
- Cong, W.; Zhang, S.; Kang, J.; Yuan, B.; Wu, H.; Zhou, X.; Tong, H.; and Mahdavi, M. 2023. Do We Really Need Complicated Model Architectures For Temporal Networks? In *International Conference on Learning Representations*.
- Fey, M.; and Lenssen, J. E. 2019. Fast Graph Representation Learning with PyTorch Geometric. In *International Conference on Learning Representations Workshop on Representation Learning on Graphs and Manifolds*.
- Gravina, A.; Lovisotto, G.; Gallicchio, C.; Bacciu, D.; and Grohfeldt, C. 2024. Long Range Propagation on Continuous-Time Dynamic Graphs. *International Conference on Machine Learning*.
- Hamilton, W. L.; Ying, R.; and Leskovec, J. 2017. Inductive representation learning on large graphs. In *International Conference on Neural Information Processing Systems*.
- Hegazy, K.; Mahoney, M.; and Erichson, N. B. 2025. Powerformer: A Transformer with Weighted Causal Attention for Time-series Forecasting.
- Huang, S.; Poursafaei, F.; Danovitch, J.; Fey, M.; Hu, W.; Rossi, E.; Leskovec, J.; Bronstein, M.; Rabusseau, G.; and Rabbany, R. 2023. Temporal Graph Benchmark for Machine Learning on Temporal Graphs. *Advances in Neural Information Processing Systems*.
- Huang, X.; Yang, Y.; Wang, Y.; Wang, C.; Zhang, Z.; Xu, J.; Chen, L.; and Vazirgiannis, M. 2022. DGraph: A Large-Scale Financial Dataset for Graph Anomaly Detection. *Advances in Neural Information Processing Systems*.
- Kazemi, S. M.; Goel, R.; Jain, K.; Kobyzhev, I.; Sethi, A.; Forsyth, P.; and Poupart, P. 2020. Representation learning for dynamic graphs: A survey. *Journal of Machine Learning Research*.
- Kipf, T. N.; and Welling, M. 2017. Semi-Supervised Classification with Graph Convolutional Networks. In *International Conference on Learning Representations*.
- Kumar, S.; Zhang, X.; and Leskovec, J. 2019. Predicting Dynamic Embedding Trajectory in Temporal Interaction Networks. In *Proceedings of the 25th ACM SIGKDD international conference on Knowledge discovery and data mining*.
- Liao, R.; Zhao, Z.; Urtasun, R.; and Zemel, R. 2019. LanczosNet: Multi-Scale Deep Graph Convolutional Networks. In *International Conference on Learning Representations*.
- Liu, C.; Yao, Z.; Zhan, Y.; Ma, X.; Pan, S.; and Hu, W. 2024. Gradformer: graph transformer with exponential decay. In *Proceedings of the Thirty-Third International Joint Conference on Artificial Intelligence*.
- Longa, A.; Lachi, V.; Santin, G.; Bianchini, M.; Lepri, B.; Lio, P.; Scarselli, F.; and Passerini, A. 2023. Graph neural networks for temporal graphs: State of the art, open challenges, and opportunities. *arXiv preprint arXiv:2302.01018*.
- Luo, Y.; and Li, P. 2022. Neighborhood-aware Scalable Temporal Network Representation Learning. *Learning on Graphs Conference*.
- Niu, P.; Zhou, T.; Wang, X.; Sun, L.; and Jin, R. 2024. Attention as Robust Representation for Time Series Forecasting.
- Poursafaei, F.; Huang, S.; Peltz, K.; and Rabbany, R. 2022. Towards better evaluation for dynamic link prediction. *Advances in Neural Information Processing Systems*.
- Press, O.; Smith, N.; and Lewis, M. 2022. Train Short, Test Long: Attention with Linear Biases Enables Input Length Extrapolation. In *International Conference on Learning Representations*.
- Rosin, G. D.; and Radinsky, K. 2022. Temporal attention for language models. *The Nations of the Americas Chapter of the Association for Computational Linguistics*.
- Rossi, E.; Chamberlain, B.; Frasca, F.; Eynard, D.; Monti, F.; and Bronstein, M. 2020. Temporal Graph Networks for Deep Learning on Dynamic Graphs. In *International Conference on Machine Learning 2020 Workshop on Graph Representation Learning*.
- Shamsi, K.; Victor, F.; Kantarcioğlu, M.; Gel, Y.; and Akcora, C. G. 2022. Chartalist: Labeled Graph Datasets for UTXO and Account-based Blockchains. In *Advances in Neural Information Processing Systems*.
- Trivedi, R.; Farajtabar, M.; Biswal, P.; and Zha, H. 2019. DyRep: Learning Representations over Dynamic Graphs. In *International Conference on Learning Representations*.
- Vaswani, A.; Shazeer, N.; Parmar, N.; Uszkoreit, J.; Jones, L.; Gomez, A. N.; Kaiser, L. u.; and Polosukhin, I. 2017. Attention is All you Need. In *Advances in Neural Information Processing Systems*. Curran Associates, Inc.
- Wang, L.; Chang, X.; Li, S.; Chu, Y.; Li, H.; Zhang, W.; He, X.; Song, L.; Zhou, J.; and Yang, H. 2021a. TCL: Transformer-based Dynamic Graph Modelling via Contrastive Learning. *Computing Research Repository*.
- Wang, Y.; Chang, Y.-Y.; Liu, Y.; Leskovec, J.; and Li, P. 2021b. Inductive Representation Learning in Temporal Networks via Causal Anonymous Walks. In *International Conference on Learning Representations*.
- Wu, Y.; Fang, Y.; and Liao, L. 2024. On the Feasibility of Simple Transformer for Dynamic Graph Modeling. *WWW*.
- Xu, D.; Ruan, C.; Korpeoglu, E.; Kumar, S.; and Achan, K. 2019. Self-attention with functional time representation learning. *Advances in neural information processing systems*.
- Xu, D.; Ruan, C.; Korpeoglu, E.; Kumar, S.; and Achan, K. 2020. Inductive representation learning on temporal graphs. In *International Conference on Learning Representations*.

Yu, L.; Sun, L.; Du, B.; and Lv, W. 2023. Towards Better Dynamic Graph Learning: New Architecture and Unified Library. *Advances in Neural Information Processing Systems*.

Yuan, Q.; Liu, Y.; Tang, Y.; Chen, X.; Zheng, X.; He, Q.; and Ao, X. 2025. Dynamic Graph Learning with Static Relations for Credit Risk Assessment. *Proceedings of the AAAI Conference on Artificial Intelligence*.

Zhang, X.; Wang, Y.; Wang, X.; and Zhang, M. 2024. Efficient Neural Common Neighbor for Temporal Graph Link Prediction. *arXiv preprint arXiv:2406.07926*.

Zheng, Y.; Yi, L.; and Wei, Z. 2025. A survey of dynamic graph neural networks. *Frontiers of Computer Science*.

## Appendix

**Appendix A:** Notations

**Appendix B:** Moment Analysis of Kernel-Weighted Time Encodings

**Appendix C:** Dataset Description and Statistics

**Appendix D:** DygFormer

**Appendix E:** Impact of Temporal Kernels on Higher-Order Moments

**Appendix F:** Baselines

**Appendix G:** Additional Experimental Details and Results

**Appendix H:** Code and Reproducibility

## Appendix A: Notations

Symbol	Description
<i>Graph and Temporal Setting</i>	
$\mathcal{G} = (\mathcal{V}, \mathcal{E}, T)$	Dynamic temporal graph
$\mathcal{V}, \mathcal{E}$	Node and edge sets
$T$	Set of event timestamps
$t_{ij}$	Timestamp of edge $(i, j)$
$\Delta t = t_i - t_{ij}$	Time elapsed since interaction
$\mathcal{N}(i)$	Temporal neighbors of node $i$
$\mathbf{e}_{ij} \in \mathbb{R}^{d_e}$	Static edge features
$\bar{\mathbf{e}}_{ij} = [\mathbf{e}_{ij} \parallel \phi(\Delta t)]$	Concatenated edge-time feature
<i>Embeddings and Attention Computation</i>	
$\mathbf{h}_i, \mathbf{h}_j \in \mathbb{R}^d$	Node embeddings
$\alpha_{ij}$	Attention from node $i$ to $j$
$d_k$	Key/query dimensionality
$\mathbf{h}'_i$	Updated embedding of node $i$
$\mathbf{W}_q, \mathbf{W}_k, \mathbf{W}_v$	Query, key, and value projection matrices
$\mathbf{W}_{\text{self}}$	Self-embedding residual weight
$\mathbf{W}_e, \mathbf{W}'_e$	Edge feature transformation matrices
<i>Temporal Modulation (KEAT)</i>	
$\psi(\Delta t)$	Temporal kernel applied to edge
$\psi(\Delta t) = \exp(-\Delta t/\sigma)$	Laplacian kernel
$\psi(\Delta t) = \exp(-\Delta t^2/\sigma^2)$	RBF kernel
$\psi(\Delta t) = \text{MLP}(\Delta t)$	Learned kernel (parametric)
$\sigma$	Temporal scale parameter (std. of $\Delta t$ )
$\psi(\Delta t) \cdot \bar{\mathbf{e}}_{ij}$	Modulated edge-time feature
<i>Series Interpretation and Expectations</i>	
$\omega$	Frequency parameter in cosine kernel
$\mathbb{E}_{\Delta t}[\cos(\omega \Delta t)]$	Expected time-frequency response
$\mathbb{E}[(\Delta t)^{2n}]$	$2n$ -th moment of time differences
$n$	Index in Taylor expansion

Table 3: Summary of Notation

## Appendix B: Moment Analysis of Kernel-Weighted Time Encodings

### B.1 Taylor Expansion of $\cos(\omega\Delta t)$

We begin by analyzing a commonly used time encoding function,  $\cos(\omega\Delta t)$ , where  $\omega$  is a frequency hyperparameter and  $\Delta t$  is the time difference. The Taylor series expansion is given by:

$$\cos(\omega\Delta t) = \sum_{n=0}^{\infty} \frac{(-1)^n (\omega\Delta t)^{2n}}{(2n)!} \quad (6)$$

Taking expectation with respect to the inter-arrival distribution  $p(\Delta t)$ , we obtain:

$$\mathbb{E}_{\Delta t}[\cos(\omega\Delta t)] = \sum_{n=0}^{\infty} \frac{(-1)^n \omega^{2n}}{(2n)!} \mathbb{E}[(\Delta t)^{2n}] \quad (7)$$

This reveals that the encoding is only sensitive to even-order moments (e.g., variance, kurtosis), and entirely insensitive to odd-order moments like the mean or skewness.

### B.2 Introducing Temporal Modulation Kernels

To enrich moment sensitivity, we consider multiplying the encoding with a temporal modulation kernel  $\psi(\Delta t)$ , such as:

- **Laplacian kernel:**  $\psi(\Delta t) = \exp(-|\Delta t|/\tau)$

Consider the kernel-modulated encoding:

$$f(\Delta t) = \psi(\Delta t) \cdot \cos(\omega\Delta t) \quad (8)$$

Both  $\psi(\Delta t)$  and  $\cos(\omega\Delta t)$  can be expressed as Taylor series:

$$\psi(\Delta t) = \sum_{m=0}^{\infty} \frac{(-\lambda)^m}{m!} (\Delta t)^m \quad (\text{e.g., exponential}) \quad (9)$$

$$\cos(\omega\Delta t) = \sum_{n=0}^{\infty} \frac{(-1)^n \omega^{2n}}{(2n)!} (\Delta t)^{2n} \quad (10)$$

Multiplying the two series yields:

$$f(\Delta t) = \left( \sum_{m=0}^{\infty} a_m (\Delta t)^m \right) \cdot \left( \sum_{n=0}^{\infty} b_n (\Delta t)^{2n} \right), \quad (11)$$

$$f(\Delta t) = \sum_{k=0}^{\infty} c_k (\Delta t)^k, \quad (12)$$

where  $a_m = \frac{(-\lambda)^m}{m!}$  and  $b_n = \frac{(-1)^n \omega^{2n}}{(2n)!}$  are the series coefficients of the kernel and encoding, respectively. The resulting coefficients  $c_k$  arise from all pairs  $(m, n)$  satisfying  $k = m + 2n$ , leading to a series expansion that includes both even and odd powers of  $\Delta t$ .

Taking expectation:

$$\mathbb{E}_{\Delta t}[f(\Delta t)] = \sum_{k=0}^{\infty} c_k \cdot \mathbb{E}[(\Delta t)^k] \quad (13)$$

This confirms that the modulated encoding incorporates contributions from all statistical moments of the inter-arrival distribution  $p(\Delta t)$ .

### B.3 Implications for Temporal Graph Models

This analysis highlights a fundamental limitation of standard encoding functions such as  $\cos(\omega\Delta t)$  or  $\sin(\omega\Delta t)$ : they are inherently blind to half of the moment spectrum. By introducing a modulation kernel  $\psi(\Delta t)$ , we recover full moment sensitivity, enabling the encoding to reflect both symmetric and asymmetric properties of the temporal distribution.

This hybrid formulation enhances the robustness of attention mechanisms to distributional shifts in  $\Delta t$  and better aligns with the non-stationary nature of real-world temporal data. It also offers theoretical justification for the kernel-weighted attention strategy employed in our model.

## Appendix C: Dataset Description and Statistics

This appendix provides full descriptions of the datasets used in our evaluation.

### Dynamic Link Prediction

For this task, experiments are conducted on eight datasets. Five from TGB (Huang et al. 2023) and three are from JODIE (Kumar, Zhang, and Leskovec 2019). Wikipedia dataset is common in both TGB and JODIE. Description of these datasets is as follows:

**tgb1-wiki**: This dataset contains information on edits made by users to Wikipedia pages. It forms a bipartite graph with users and wiki pages as nodes. Each edge is associated with features derived from the edits, along with corresponding timestamps.

**tgb1-review**: This dataset contains reviews of Amazon products in the electronics category, collected from 1997 to 2018. Here, users and products form nodes. Ratings range from 1 to 5. It forms a weighted bipartite graph.

**tgb1-coin**: This dataset contains cryptocurrency transaction data (Shamsi et al. 2022) from April 1st, 2022 to November 1st, 2022. Nodes represent wallet addresses, and edges capture fund transfers over time.

**tgb1-comment**: This dataset is a Reddit interaction graph where users are nodes and comments represent edges. It spans the years 2005 to 2010.

**tgb1-flight**: This dataset represents a daily international flight network, where nodes are airports and edges correspond to scheduled flights annotated with metadata. Node features include information about the airports. The dataset spans the years 2019 to 2022.

The **tgb1** dataset statistics is provided in Table 4.

Additionally, we include following four datasets from JODIE (Kumar, Zhang, and Leskovec 2019)<sup>4</sup> for link prediction. Note that **tgb1-wiki** and **jodie-wiki** are the same datasets. Description of the remaining datasets is as follows:

**jodie-reddit**: This public dataset consists of one month of user posts made across various subreddits.

<sup>4</sup>Dataset loader is from: [https://github.com/pyg-team/pytorch-geometric/blob/master/torch\\_geometric/datasets/jodie.py](https://github.com/pyg-team/pytorch-geometric/blob/master/torch_geometric/datasets/jodie.py).

Task	Scale	Dataset	#Nodes	#Edges	#Steps	Surprise	# Negatives
Link (t <sub>gbl</sub> )	Small	t <sub>gbl</sub> -wiki	9,227	157,474	152,757	0.108	999
	Small	t <sub>gbl</sub> -review	352,637	4,873,540	6,865	0.987	100
	Medium	t <sub>gbl</sub> -coin	638,486	22,809,486	1,295,720	0.120	20
	Large	t <sub>gbl</sub> -comment	994,790	44,314,507	30,998,030	0.823	20
	Large	t <sub>gbl</sub> -flight	18,143	67,169,570	1,385	0.024	20

Table 4: Dataset statistics from TGB across link prediction and node classification tasks. Surprise values are taken from (Huang et al. 2023). # Negatives is the number of negatives used for one positive link in the MRR calculation.

Dataset	#Nodes	#Edges	# Negatives
jodie-reddit	6,509	25,470	1
jodie-wiki	9,227	157,474	1
jodie-mooc	7,144	411,749	1
jodie-lastfm	1,980	1,293,103	1

Table 5: Statistics of jodie-datasets used for link prediction. For these datasets, one negative link is used against one positive link, making it binary classification problem.

**jodie-mooc**: This public dataset consists of student actions on a MOOC online course, such as viewing videos, submitting answers, and other interactions.

**jodie-lastfm**: This public dataset contains one month of user listening activity, indicating which songs were listened to by which users.

Table 5 summarizes the statistics of jodie-datasets.

## Dynamic Node Classification

The experiments for this task are conducted on five datasets. Four of these are from (Huang et al. 2023), namely, t<sub>gbn</sub>-trade, t<sub>gbn</sub>-genre, t<sub>gbn</sub>-reddit and t<sub>gbn</sub>-token. Apart from TGB, we include DGraphFin dataset (Huang et al. 2022), which contains financial scenarios. Description of these datasets is as follows:

**t<sub>gbn</sub>-trade**: This dataset represents the international agricultural trade network among UN nations from 1986 to 2016, where nodes are countries and edges indicate the annual total trade value of agricultural products.

**t<sub>gbn</sub>-genre**: This is a weighted bipartite interaction network between users and music genres, where edges indicate that a user listened to a genre at a specific time. Edge weights reflect the percentage association of a song with the given genre.

**t<sub>gbn</sub>-reddit**: This is a user–subreddit interaction network where both users and subreddits are nodes. Edges represent user posts on subreddits at specific times, spanning from 2005 to 2019. The task is to predict a user’s interaction frequency with subreddits in the following week.

**t<sub>gbn</sub>-token**: This is a user–token transaction network where both users and cryptocurrency tokens are nodes. Edges represent token transfers from users, with weights indicating the transaction amount. Due to weight disparity, edge weights are log-normalized. The task is to predict a user’s interaction frequency with different tokens in the next

week.

**dgraph-fin**: A directed, unweighted dynamic graph representing a social network among users of Finvolution Group, where each node is a user and edges denote emergency contact relationships. Edges carry encrypted timestamps indicating when the contact was added. The task is to detect fraudulent users (Class 1) versus normal users (Class 0), using node features and temporal graph structure.

Statistics for the t<sub>gbn</sub> datasets are presented in Table 6, while those for DGraphFin are shown in Table 7.

## Temporal Drift in Inter-Arrival Distributions.

Figure 9 presents the inter-arrival time distributions  $p(\Delta t)$  across 12 temporal graph datasets used in our experiments. We evaluate five link prediction datasets from the TGB benchmark (t<sub>gbl</sub>-wiki, t<sub>gbl</sub>-review, t<sub>gbl</sub>-coin, t<sub>gbl</sub>-comment, and t<sub>gbl</sub>-flight) and four node classification datasets (t<sub>gbn</sub>-trade, t<sub>gbn</sub>-genre, t<sub>gbn</sub>-token, and t<sub>gbn</sub>-reddit) from the same benchmark. To further assess the generalization capability of our method KEAT, we additionally consider four datasets from the JODIE paper—jodie-wiki, jodie-mooc, jodie-reddit, and jodie-lastfm—for link prediction, using the original evaluation setup defined in JODIE. Notably, jodie-wiki and t<sub>gbl</sub>-wiki represents the same dataset. For each dataset, we compare the inter-arrival distribution  $p(\Delta t)$  between the training and validation sets. These visualizations reveal frequent distribution shifts, with validation distributions often exhibiting heavier tails or shifted modes. This motivates our use of temporally robust mechanisms, such as kernel-based attention, which mitigate sensitivity to higher-order temporal statistics that are not consistent across splits.

## Spectral Density Plots

The figure 3 represents the spectral density plots for different datasets on which our experiments were performed. Let  $P_f$  denote the probability associated with each frequency component of the signal at the node level, and  $M_f$  represent the magnitude of the corresponding frequency component in the fast Fourier Transform (FFT) spectrum at the node level. Then the formulation for the entropy is given as  $H(P) = -\sum_f P_f \log P_f$ .

We arrive at there values of spectral entropy on a node level and plot the kernel density estimation (KDE) plot for all nodes of each dataset. We first take the timestamps of

Task	Scale	Dataset	#Nodes	#Edges	#Steps	Surprise
Node (tgbn)	Small	tgbn-trade	255	468,245	32	0.023
	Medium	tgbn-genre	1,505	17,858,395	133,758	0.005
	Large	tgbn-reddit	11,766	27,174,118	21,889,537	0.013
	Large	tgbn-token	61,756	72,936,998	2,036,524	0.014

Table 6: Dataset statistics from TGB across node classification tasks. Surprise values are taken from (Huang et al. 2023).

Dataset	#Nodes	#Edges
DGraphFin	3,700,550	4,300,999

Table 7: Statistics of DGraphFin used for node classification.

interaction on a node wise level for a particular dataset under consideration. Once the series of timestamps are noted, the corresponding FFT is taken at a node wise level. These FFTs represent magnitudes/ or intensities of different signals. Here the  $P_f$  for a particular signal is calculated as  $P_f = M_f / \sum(M_f)$ . Once this  $P_f$  is calculated for each signal for each node we calculate spectral entropy for each node as mentioned in the expression before. Ideally a purely periodic node would have only one signal leading to 0 spectral entropy. Hence, lower is the value of spectral entropy greater is the degree of periodicity.

Lower entropy reflects greater periodicity in the data, whereas higher entropy denotes increased randomness. Based on the spectral density plots in Figure 3, the datasets can be ranked by their level of periodicity, from most to least periodic, as follows: tgb1-review, tgb1-coin, tgb1-wiki, tgb1-comment, and tgb1-flight. This observation shows that many datasets do not display strong periodic patterns. Therefore, relying only on time encodings, which primarily aim to capture periodic behavior, may not be adequate. This motivates the design of KEAT, which enables effective temporal modeling by leveraging edge-aware attention to capture both periodic and non-periodic temporal dynamics.

## Appendix D: DyGFormer

In DyGFormer (Yu et al. 2023), for each interaction  $(i, j, t_{ij})$ , the temporal neighborhoods  $\mathcal{N}(i)$  and  $\mathcal{N}(j)$  of length  $L$  each, are divided into  $\frac{L}{L_p}$  non-overlapping patches, each containing  $L_p (< L)$  interactions. For each patch  $\mathcal{P} = \{(u_k, v_k, t_k)\}_{k=1}^{L_p}$ , node features, edge features, and time encodings across the patch are concatenated as  $\mathbf{h}_{\text{flat}} \in \mathbb{R}^{L_p \cdot d_h}$ ,  $\mathbf{e}_{\text{flat}} \in \mathbb{R}^{L_p \cdot d_e}$ , and  $\phi_{\text{flat}} \in \mathbb{R}^{L_p \cdot d_t}$ . These are projected independently as :

$$\tilde{\mathbf{h}} = \mathbf{W}_h \mathbf{h}_{\text{flat}}, \quad \tilde{\mathbf{e}} = \mathbf{W}_e \mathbf{e}_{\text{flat}}, \quad \tilde{\phi} = \mathbf{W}_t \phi_{\text{flat}},$$

where  $\mathbf{W}_h \in \mathbb{R}^{d' \times L_p \cdot d_h}$ ,  $\mathbf{W}_e \in \mathbb{R}^{d' \times L_p \cdot d_e}$ , and  $\mathbf{W}_t \in \mathbb{R}^{d' \times L_p \cdot d_t}$ . The final representation for each patch is

$$\mathbf{z}_{\mathcal{P}} = [\tilde{\mathbf{h}} \parallel \tilde{\mathbf{e}} \parallel \tilde{\phi}] \in \mathbb{R}^{3d'}$$

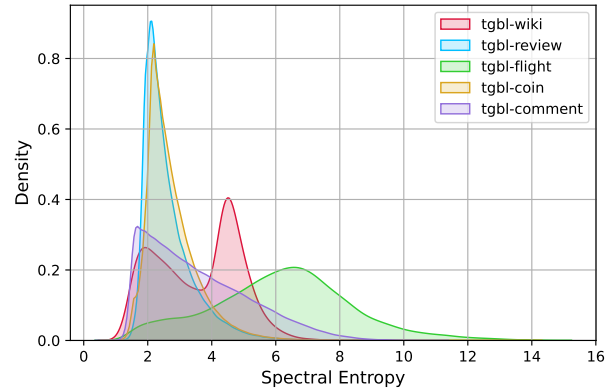


Figure 3: Spectral density for tgb1-datasets illustrating the nature of periodicity.

To incorporate KEAT, for each patch we define a representative patch timestamp  $t_{\text{patch}} = \frac{1}{L_p} \sum_{k=1}^{L_p} t_k$ , and scale the query and key vectors as:

$$\mathbf{q} = \exp(t_{\text{patch}}) \cdot \mathbf{W}_q \mathbf{z}_{\mathcal{P}}, \quad \mathbf{k} = \exp(-t_{\text{patch}}) \cdot \mathbf{W}_k \mathbf{z}_{\mathcal{P}},$$

leading to an attention score where the edge features are modulated by a temporal kernel  $\exp(t_{\text{patch}}^{(p)} - t_{\text{patch}}^{(q)})$ . This introduces a directional temporal bias by asymmetrically scaling the queries and keys based on patch timestamps. As a result, the attention mechanism becomes sensitive to temporal dynamics without modifying DyGFormer's architecture.

## Appendix E: Impact of Temporal Kernels on Higher-Order Moments

In TGNs, time encodings such as  $f(t) = \sum_{n=0}^{\infty} c_n t^n$  are often used to capture fine-grained timing patterns. However, higher-order moments  $\mathbb{E}[t^n]$  can become unstable under temporal distribution shift (e.g., when test timestamps differ from training), especially in long-tailed distributions (see Figure 9). To mitigate this, we introduce a temporal kernel  $K(t_i, t_j) = \exp\left(-\frac{|t_i - t_j|}{C}\right)$  that effectively attenuates large  $t$ , suppressing higher-order moments in time encoding functions.

**Theorem 2** Let  $p(t)$  be a probability density function supported on  $[0, \infty)$  such that  $\mathbb{E}[t^n] < \infty$  and  $\mathbb{E}[\psi(t)t^n] < \infty$  for all  $n \geq 0$ , where  $\psi(t)$  is a non-negative, monotonically decreasing kernel function. Let  $\phi(t) = \sum_{n=0}^{\infty} c_n t^n$  be an

analytic time encoding function with coefficients  $\{c_n\}$ . Define the kernel-to-base ratio for each moment order  $n$  as:

$$R_n = \frac{\mathbb{E}[\psi(t)t^n]}{\mathbb{E}[t^n]}, \quad \text{with } R_0 = \mathbb{E}[\psi(t)].$$

Then, the sequence  $\{R_n\}_{n=0}^{\infty}$  is strictly decreasing and converges to zero:  $\lim_{n \rightarrow \infty} R_n = 0$ . As a result, the expected kernel-weighted time encoding  $\mathbb{E}[\psi(t) \cdot \phi(t)]$  becomes increasingly dominated by lower-order terms  $\phi$ . This formulation naturally extends to expectations of the form  $\mathbb{E}[\psi(t) \cdot \bar{e}_{ij}]$ , as used in Equations 4 and 5.

**Proof.** To show monotonicity, consider the ratio:

$$\frac{R_{n+1}}{R_n} = \frac{\mathbb{E}[t^{n+1}\psi(t)] \cdot \mathbb{E}[t^n]}{\mathbb{E}[t^n\psi(t)] \cdot \mathbb{E}[t^{n+1}]}.$$

Both numerator and denominator are expectations involving  $t^k$  under two different distributions: one weighted by  $\psi(t)$  and one unweighted. Since  $\psi(t)$  is a non-negative, strictly decreasing function, it downweights larger values of  $t$ , leading to:

$$\frac{\mathbb{E}[t^{n+1}\psi(t)]}{\mathbb{E}[t^n\psi(t)]} < \frac{\mathbb{E}[t^{n+1}]}{\mathbb{E}[t^n]}.$$

Hence,  $R_{n+1} < R_n$ .

To prove convergence to zero, observe that  $\psi(t) \leq \psi(0)$  and decays faster than any polynomial growth in  $t$ . Thus:

$$\lim_{n \rightarrow \infty} \frac{\mathbb{E}[t^n\psi(t)]}{\mathbb{E}[t^n]} = 0,$$

as the numerator decays faster than the denominator. Therefore,  $\lim_{n \rightarrow \infty} R_n = 0$ .

This implies that for the analytic expansion  $\phi(t) = \sum c_n t^n$ , we have:

$$\mathbb{E}[\psi(t) \cdot \phi(t)] = \sum_{n=0}^{\infty} c_n \mathbb{E}[\psi(t)t^n] = \sum_{n=0}^{\infty} c_n R_n \mathbb{E}[t^n],$$

where the coefficients  $R_n$  decay rapidly, suppressing higher-order moments.

A visual illustration of higher-order moment suppression is shown in Figure 4.

## Variance Reduction in KEAT

### Theorem 3 (Variance Reduction via Temporal Kernel)

In the KEAT formulation, the attention logits for node  $i$  with neighbor  $j$  take the form:

$$s_{ij}^{(K)} := \mathbf{q}_i^{\top} \left( \mathbf{k}_j + \psi(\Delta t_{ij}) \cdot \mathbf{k}_{ij}^{(\text{edge})} \right) = X_j + \psi_{ij} Y_j,$$

where:

- $X_j := \mathbf{q}_i^{\top} \mathbf{k}_j$  is the node-to-node interaction term,
- $Y_j := \mathbf{q}_i^{\top} \mathbf{k}_{ij}^{(\text{edge})}$  captures edge-specific contributions,
- $\psi(\cdot)$  is a temporal kernel (e.g., exponential decay), and  $\psi_{ij} := \psi(\Delta t_{ij}) \in (0, 1]$  is its value for the edge from  $j$  to  $i$ .

Assume  $\{(X_j, Y_j)\}$  are i.i.d. with variances  $\sigma_X^2$ ,  $\sigma_Y^2$ , and correlation  $\rho \in [-1, 1]$ . Then the variance of the kernel-modulated logits satisfies:

$$\text{Var}[s_{ij}^{(K)}] \leq \text{Var}[s_{ij}^{(0)}] \quad \text{whenever} \quad \sigma_Y(1 + \psi_{ij}) \geq 2\sigma_X.$$

Thus, the temporal kernel suppresses variance from edge-based noise, yielding more stable attention logits.

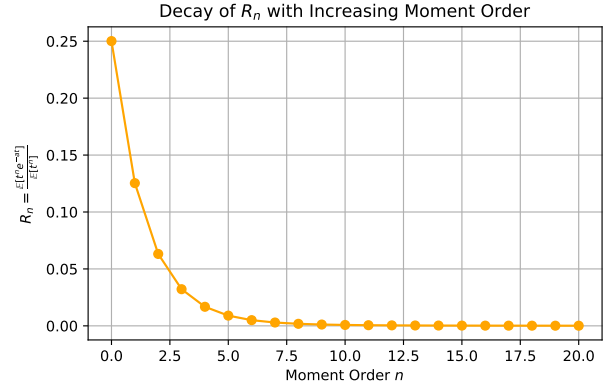


Figure 4: Decay of the ratio  $R_n = \frac{\mathbb{E}[t^n e^{-at}]}{\mathbb{E}[t^n]}$  for increasing moment order  $n$ , where  $t \sim \text{Exp}(1)$ . This demonstrates how higher-order moments are increasingly suppressed under exponential kernel weighting.

**Proof.** Let the kernel-modulated and unmodulated logits be:

$$s_{ij}^{(K)} = X_j + \psi_{ij} Y_j, \quad s_{ij}^{(0)} = X_j + Y_j,$$

where  $\psi_{ij} := \psi(\Delta t_{ij}) \in (0, 1]$ .

We compute the variances under the assumption that  $(X_j, Y_j)$  are i.i.d. with variances  $\sigma_X^2, \sigma_Y^2$ , and correlation  $\rho \in [-1, 1]$ :

$$\begin{aligned} \text{Var}[s_{ij}^{(K)}] &= \text{Var}[X_j + \psi_{ij} Y_j] \\ &= \sigma_X^2 + \psi_{ij}^2 \sigma_Y^2 + 2\psi_{ij}\rho\sigma_X\sigma_Y \end{aligned}$$

$$\text{Var}[s_{ij}^{(0)}] = \sigma_X^2 + \sigma_Y^2 + 2\rho\sigma_X\sigma_Y$$

Let  $\Delta := \text{Var}[s_{ij}^{(0)}] - \text{Var}[s_{ij}^{(K)}]$ . Then:

$$\begin{aligned} \Delta &= (\sigma_X^2 + \sigma_Y^2 + 2\rho\sigma_X\sigma_Y) \\ &\quad - (\sigma_X^2 + \psi_{ij}^2 \sigma_Y^2 + 2\psi_{ij}\rho\sigma_X\sigma_Y) \\ &= \sigma_Y^2(1 - \psi_{ij}^2) + 2\rho\sigma_X\sigma_Y(1 - \psi_{ij}). \end{aligned}$$

Factoring:

$$\Delta = (1 - \psi_{ij}) [\sigma_Y^2(1 + \psi_{ij}) + 2\rho\sigma_X\sigma_Y].$$

Define the bracketed expression as:

$$B := \sigma_Y^2(1 + \psi_{ij}) + 2\rho\sigma_X\sigma_Y.$$

Since  $1 - \psi_{ij} > 0$ , the sign of  $\Delta$  depends on  $B$ . In the worst case ( $\rho = -1$ ), we have:

$$B_{\min} = \sigma_Y^2(1 + \psi_{ij}) - 2\sigma_X\sigma_Y.$$

Thus,  $\Delta \geq 0$  (i.e., variance is reduced) whenever:

$$\sigma_Y(1 + \psi_{ij}) \geq 2\sigma_X.$$

This completes the proof.

## Extension: Correlated Neighbor Terms

Even when the i.i.d. assumption on neighbor pairs  $(X_j, Y_j)$  is relaxed, we can still show that incorporating the temporal kernel leads to a reduction in the variance of the aggregated attention logits under mild conditions. In realistic temporal graphs, interactions from neighbors may exhibit correlations due to structural proximity or temporal locality. The following extension demonstrates that variance reduction continues to hold so long as these correlations are non-negative.

Let the attention logits in KEAT be given by

$$s_{ij}^{(K)} := X_j + \psi_{ij} Y_j,$$

where  $\psi_{ij} := \psi(\Delta t_{ij}) \in (0, 1]$ , and define the neighborhood-averaged logit:

$$\bar{s}_i^{(K)} := \frac{1}{|\mathcal{N}(i)|} \sum_{j \in \mathcal{N}(i)} s_{ij}^{(K)}.$$

Assume that for all  $j \neq l$ , the cross-covariances satisfy:

$$\text{Cov}[Y_j, Y_l] \geq 0, \quad \text{Cov}[X_j, Y_l] \geq 0, \quad \text{Cov}[Y_j, X_l] \geq 0.$$

Then,

$$\text{Var}[\bar{s}_i^{(K)}] \leq \text{Var}[\bar{s}_i^{(0)}].$$

**Proof.** Let  $s_{ij}^{(0)} := X_j + Y_j$ . The variance of the neighborhood-averaged logit is:

$$\text{Var}[\bar{s}_i^{(K)}] = \frac{1}{n^2} \sum_{j,l} \text{Cov}[X_j + \psi_{ij} Y_j, X_l + \psi_{il} Y_l].$$

Taking the difference from the unmodulated case and expanding yields:

$$\begin{aligned} \Delta &:= \text{Var}[\bar{s}_i^{(0)}] - \text{Var}[\bar{s}_i^{(K)}] \\ &= \frac{1}{n^2} \sum_{j,l} [(1 - \psi_{ij}\psi_{il})\text{Cov}[Y_j, Y_l] \\ &\quad + (1 - \psi_{ij})\text{Cov}[X_j, Y_l] \\ &\quad + (1 - \psi_{il})\text{Cov}[Y_j, X_l]]. \end{aligned}$$

Each term in the sum is non-negative under the stated covariance conditions and  $\psi_{ij} \in (0, 1]$ , implying  $\Delta \geq 0$ .

**Remark.** This generalization shows that the variance reduction effect of KEAT holds even in the presence of correlated or temporally clustered neighbors, so long as the correlations are non-negative. This setting captures realistic temporal graph phenomena like structurally similar interactions. The temporal kernel acts as a soft attention prior that dampens noisy or high-variance edge contributions, improving the stability of attention logits under broader assumptions.

## Different Types of Kernels

Figure 5 illustrates the behavior of three temporal kernels used in KEAT to modulate edge time interactions. The Laplacian and RBF kernels apply fixed decay functions. The Laplacian kernel exhibits an exponential drop with a linear rate of decay, while the RBF kernel shows a sharper and

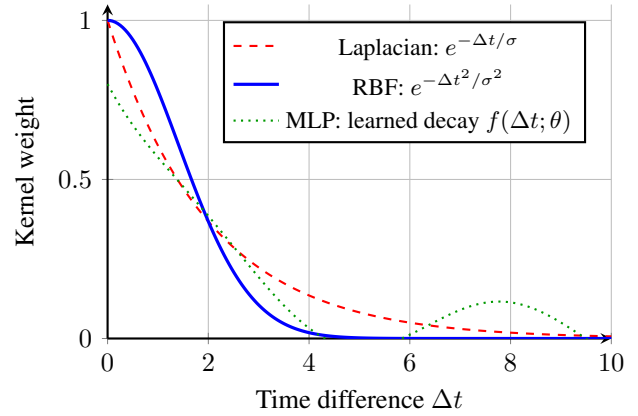


Figure 5: Comparison of temporal kernels used in KEAT for edge modulation. Laplacian and RBF apply fixed exponential decays, while the MLP-based kernel learns a flexible decay pattern from data, allowing richer temporal biasing.

symmetric decay. These fixed forms are effective for modeling simple recency-based interactions. In contrast, the MLP-based kernel learns its decay pattern directly from data, allowing it to capture complex and potentially non-monotonic temporal dependencies. This learnable flexibility enables KEAT to better adapt to diverse temporal structures in dynamic graphs.

## Appendix F: Baselines

Table 8 describes the ranks for each baseline on different `tgb1` link prediction datasets. We select TNCN, TGN, CTAN, and DyGFormer as our primary baselines due to their consistently strong performance across multiple datasets in the TGB benchmark<sup>5</sup>. These models represent a diverse set of temporal graph architectures and provide competitive results in both average ranking and ranking MRR. In contrast, several other methods exhibit poor generalization, scalability (highlighted by red cells in Table 8) or lack robustness across datasets, often missing scores and receiving penalized ranks. To maintain clarity and focus in our evaluations, we omit these underperforming models from detailed analysis.

## Appendix G: Additional Experimental Details and Results

### Implementation Details

We employ the Adam optimizer with a learning rate of  $1 \times 10^{-4}$ , a batch size of 200, and dimensionality of 100 for embeddings, memory, and time encodings. We apply early stopping with a tolerance of  $1 \times 10^{-6}$  and a patience of 5 epochs. For the WIKI dataset, we increase the number of training epochs to 200 and set the early stopping patience to 25, owing to its smaller size. All models are trained over 5 random seeds (1 through 5), and we report the mean

<sup>5</sup>[https://tgb.complexdatalab.com/docs/leader\\_linkprop/](https://tgb.complexdatalab.com/docs/leader_linkprop/)

Method	wiki	review	coin	comment	flight	Avg Rank ↓	Ranking MRR ↑
TNCN	3	3	1	1	1	1.8	0.733
TGN	10	5	4	4	2	5.0	0.260
CTAN	5	2	3	2	17	5.8	0.318
DyGFormer	1	7	2	3	17	6.0	0.407
EdgeBank <sub>tw</sub>	6	15	5	6	4	7.2	0.170
DyRep	16	8	6	5	3	7.6	0.178
EdgeBank <sub>∞</sub>	7	16	7	7	5	8.4	0.138
NAT	2	6	17	17	17	11.8	0.169
CAWN	4	10	17	17	17	13.0	0.105
GraphMixer	15	1	17	17	17	13.4	0.249
EGCNo (UTG)	9	9	17	17	17	13.8	0.080
TGAT	14	4	17	17	17	13.8	0.100
HTGN (UTG)	8	13	17	17	17	14.4	0.076
GCN (UTG)	12	12	17	17	17	15.0	0.069
TCL	13	11	17	17	17	15.0	0.069
GCLSTM (UTG)	11	14	17	17	17	15.2	0.068

Table 8: Ranking of link prediction methods on TGB benchmark datasets. Missing scores are penalized with rank 17 and highlighted in red. Numbers are taken from TGB link prediction leaderboard (Huang et al. 2023) as on 4th Aug 2025.

Node Mod.	Edge Mod.	Val MRR	Test MRR
✓	✗	$0.374 \pm 0.163$	$0.344 \pm 0.169$
✓	✓	$0.364 \pm 0.021$	$0.360 \pm 0.024$
✗	✓	<b><math>0.515 \pm 0.053</math></b>	<b><math>0.474 \pm 0.031</math></b>
✗	✗	$0.411 \pm 0.074$	$0.391 \pm 0.064$

Table 9: Ablation of kernel modulation on nodes and edges. Results are reported as MRR (mean  $\pm$  std) on the `tgb1-wiki` dataset.

and standard deviation of the evaluation metrics. All experiments are conducted on an Ubuntu system equipped with an NVIDIA A100 80GB GPU and 128 GB of RAM.

In KEAT-TGN, the official implementation of TGN<sup>6</sup> in TGB (Huang et al. 2023) is used. For DyGFormer, we use the official implementation provided by the authors<sup>7</sup>. For the JODIE datasets, we use the implementation available in PyTorch Geometric<sup>8</sup>. For the DGraphFin dataset, we adopt the publicly available implementation of GEARsage<sup>9</sup>.

**Hyperparameters.** As KEAT is designed to be lightweight and plug-and-play, we retain the exact hyperparameters used by the respective baseline models without any additional tuning. This ensures a fair comparison and highlights the compatibility of KEAT with existing architectures. The only additional hyperparameter introduced by KEAT is the training set standard deviation ( $\sigma$ ), which is used for kernel modulation and is directly computed and reported in the code for reproducibility.

<sup>6</sup><https://github.com/shenyangHuang/TGB/tree/main>

<sup>7</sup>[https://github.com/yule-BUAA/DyGLib\\_TGB](https://github.com/yule-BUAA/DyGLib_TGB)

<sup>8</sup>[https://github.com/pyg-team/pytorch\\_geometric/blob/master/torch\\_geometric/datasets/jodie.py](https://github.com/pyg-team/pytorch_geometric/blob/master/torch_geometric/datasets/jodie.py)

<sup>9</sup><https://github.com/storyandwine/GEARsage-DGraphFin>

## Effect of Node and Edge Modulation

We analyze the contribution of kernel-based modulation on node vs. edge representations (Table 9, `tgb1-wiki`). Edge modulation alone yields the best performance: test MRR of  $0.474 \pm 0.031$ . In contrast, modulating only node features results in lower performance and higher variance. Combining both is better than node-only, but still inferior to edge-only. These results suggest that temporal modulation at the edge level is more effective, likely because edges directly influence message passing and modulate attention scores.

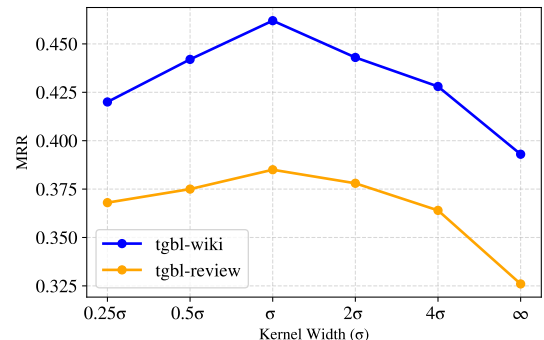


Figure 6: Kernel Width  $\sigma$  sensitivity for `tgb1-wiki`

## Kernel Width Sensitivity

In Figure 6, we analyze the robustness of KEAT under the Laplacian kernel by varying the kernel width  $\lambda$  relative to the standard deviation  $\sigma$  of time differences in the training set. As shown in the table, the mean reciprocal rank (MRR) improves as  $\lambda$  increases, peaking when  $\lambda = \sigma$  with values of 0.474 on `wiki` and 0.385 on `review`. Both smaller ( $0.25\sigma$ ,  $0.5\sigma$ ) and larger ( $2\sigma$ ,  $4\sigma$ ,  $\infty$ ) values lead to lower MRR. We have used  $\sigma > 5000$  for  $\infty$  in the code. This

Method	Split	tgb1-flight
EdgeBank <sub>tw</sub>	Val	0.363
	Test	0.387
EdgeBank <sub>∞</sub>	Val	0.166
	Test	0.167
DyRep	Val	0.573 ± 0.013
	Test	0.556 ± 0.014
TGN	Val	0.731 ± 0.010
	Test	0.705 ± 0.020
KEAT-TGN	Val	0.747 ± 0.013
	Test	<b>0.738 ± 0.022</b>
Improvement	Test	+3.30%

Table 10: Dynamic link prediction results on tgb1-flight using MRR metric.

suggests that setting  $\lambda$  close to  $\sigma$  provides an effective balance between emphasizing recent interactions and retaining longer-term dependencies, showcasing KEAT’s robustness to kernel width choice.

## Understanding Ranking in MRR

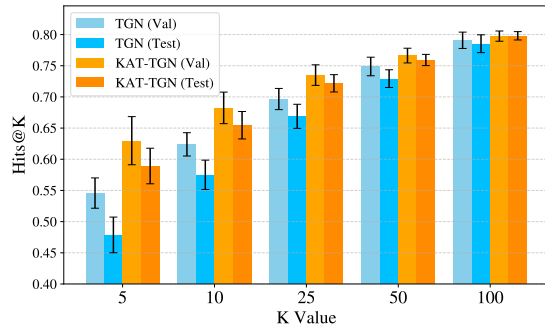


Figure 7: Hits@K for tgb1-wiki

To better interpret the ranking of predicted links beyond the MRR metric, we evaluate performance using Hits@K on the tgb1-wiki dataset for various cutoff values of  $K$ . As shown in Figure 7, our model **KEAT-TGN** consistently outperforms the baseline **TGN** across all  $K$  values, both on the validation and test sets. For instance, on the test set, KEAT-TGN achieves a Hits@10 of 65.46%, compared to 57.51% for TGN. This consistent improvement demonstrates that KEAT not only improves average ranking (as captured by MRR), but also ranks more correct links among the top- $K$  predictions, enhancing practical utility in retrieval settings.

## Results on tgb1-flight (Link Prediction)

On the tgb1-flight dataset, KEAT-TGN achieves the best performance, improving over the TGN baseline by 3.30% in MRR on the test set (0.738 vs. 0.705). Refer Table 10 for results. This demonstrates the effectiveness of KEAT

Dataset	Model	Val	Test
tgbn-trade	TGN	0.395 ± 0.002	0.374 ± 0.001
	KEAT-TGN	<b>0.464 ± 0.006</b>	<b>0.427 ± 0.010</b>
tgbn-genre	TGN	0.403 ± 0.010	0.367 ± 0.058
	KEAT-TGN	<b>0.420 ± 0.003</b>	<b>0.420 ± 0.002</b>
tgbn-reddit	TGN	<b>0.379 ± 0.004</b>	0.315 ± 0.020
	KEAT-TGN	0.372 ± 0.002	<b>0.317 ± 0.001</b>
tgbn-token	TGN	0.189 ± 0.005	0.141 ± 0.006
	KEAT-TGN	<b>0.194 ± 0.008</b>	<b>0.152 ± 0.018</b>
		Gain	+0.50% +1.1%

Table 11: Node classification performance (NDCG@10).

in enhancing temporal modeling without altering the backbone architecture. Compared to earlier methods like DyRep and EdgeBank, KEAT-TGN yields significantly higher accuracy. Additionally, while DyGFormer results are not reported here due to severe scalability issues, requiring over 24 hours to complete a single training epoch, KEAT-TGN remains efficient and practical for large-scale temporal graphs.

## Results on jodie-dataset (Link Prediction)

Table 12 presents dynamic link prediction performance on the four jodie datasets. We compare KEAT-TGN with the baseline TGN across multiple metrics, including binary cross-entropy loss, average precision (AP), and area under the ROC curve (AUC), on both validation and test sets. KEAT-TGN consistently improves upon TGN across all datasets and metrics. For example, on jodie-wiki, KEAT-TGN achieves a lower loss (0.3895 vs. 0.4065) and higher test AP (0.9660 vs. 0.9593), demonstrating better predictive performance. The improvements are particularly notable on datasets such as jodie-lastfm, where KEAT-TGN yields a significant gain in test AP (0.7438 vs. 0.6193), highlighting its ability to generalize well even in sparse user-item interaction settings. These results underscore the effectiveness of our kernelized temporal attention mechanism in enhancing the link prediction capability of the base TGN model.

**Interpretability and Temporal Precision.** As discussed in the main paper, KEAT enables time-aware edge modulation that results in temporally precise and context-sensitive attention distributions. In Appendix Figure 10 and Figure 11, we visualize attention weights over neighbors across varying  $\Delta t$ , showing how KEAT produces sharp transitions in focus that align with temporal relevance. This contrasts with standard attention mechanisms that often produce flattened or ambiguous weights. The resulting heatmaps demonstrate KEAT’s improved interpretability: the model precisely adjusts its attention as edge timestamps become older, preserving temporal fidelity and offering intuitive explanations of which past interactions are deemed important. This clarity in attention evolution enhances both transparency and analytical utility for downstream applications. To further support this, we include two additional examples

with varied attention behaviors (see Figures 12,13 for second example and Figures 14,15 for third example).

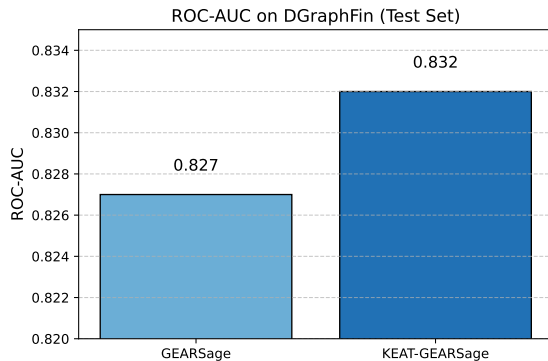


Figure 8: Test ROC-AUC scores on DGraphFin for node classification.

### Results on DGraphFin (Node Classification)

The ROC-AUC scores on the DGraphFin test set clearly indicate (see Figure 8) that KEAT-GEARsage outperforms the base GEARsage model, achieving a higher score of 0.832 compared to 0.827. This improvement demonstrates KEAT’s ability to enhance temporal modeling by better leveraging time-dependent edge information. The gain highlights KEAT’s effectiveness in capturing subtle temporal cues essential for fraud detection in dynamic financial networks.

**Time Encoding Ablation.** We evaluate the effect of KEAT across different time encoding strategies on the `tgb1-wiki`, `tgb1-review` and `tgb1-coin` datasets. As shown in Table 13, incorporating KEAT consistently improves performance across both datasets and models. For instance, GraphMixer with KEAT achieves a test MRR of 0.409 on `tgb1-review` and 0.714 on `tgb1-coin`, outperforming the baseline variants without KEAT. Similar trends are observed with TGN/TGAT models, where KEAT yields consistent gains over the default time encodings. Notably, we do not include results for LETe on `tgb1-review` and `tgb1-coin`, as it requires significantly more parameters and memory to train as shown in Table 14, which hinders its scalability for these benchmarks.

### Model Parameters

Table 14 compares trainable parameter counts across various time encoding strategies when used with the TGN backbone. While GraphMixer relies on non-trainable, fixed encodings and thus has slightly fewer parameters, it lacks the flexibility to adapt temporal patterns. The standard TGN/TGAT introduces minimal parameter overhead for time encoding (+200). LeTE-based approaches add more trainable parameters depending on the modeling strategy, with the highest cost for fully learned Fourier or Spline encodings. This demonstrates that TGN allows efficient parameter sharing

and modular integration of expressive time encodings, striking a balance between model capacity and learnability.

### Appendix H: Code and Reproducibility

To support reproducibility and fair comparison, we release our complete codebase, including training and evaluation scripts, under an anonymous folder in supplementary zip. The code includes instructions, dataset links, and configuration files to replicate experiments presented in this paper. We ensure that the released code adheres to double-blind review standards and will be made public upon acceptance.

Dataset	Method	Loss $\downarrow$	Val AP $\uparrow$	Val AUC $\uparrow$	Test AP $\uparrow$	Test AUC $\uparrow$
jodie-wiki	TGN	0.4065	0.9686	0.9659	0.9593	0.9575
	KEAT-TGN	<b>0.3895</b>	<b>0.9733</b>	<b>0.9703</b>	<b>0.9660</b>	<b>0.9634</b>
jodie-reddit	TGN	0.6876	0.9185	0.9147	0.9190	0.9149
	KEAT-TGN	<b>0.6807</b>	<b>0.9264</b>	<b>0.9219</b>	<b>0.9213</b>	<b>0.9166</b>
jodie-mooc	TGN	0.5550	0.8626	0.8875	0.8477	0.8794
	KEAT-TGN	<b>0.5420</b>	<b>0.8771</b>	<b>0.8991</b>	<b>0.8637</b>	<b>0.8898</b>
jodie-lastfm	TGN	0.9760	0.7887	0.7891	0.6193	0.6245
	KEAT-TGN	<b>0.9719</b>	<b>0.7968</b>	<b>0.7939</b>	<b>0.7438</b>	<b>0.7420</b>

Table 12: Link prediction results on jodie-datasets, using one negative sample per test edge. The model is trained with binary cross-entropy loss, and performance is reported using average precision (AP) and area under the curve (AUC). The implementation follows the `pytorch-geometric` framework.

Time Encoding	Model	tgbl-wiki		tgbl-review		tgbl-coin	
		Val	Test	Val	Test	Val	Test
GraphMixer	w/o KEAT	$0.477 \pm 0.041$	$0.432 \pm 0.061$	$0.337 \pm 0.007$	$0.404 \pm 0.008$	$0.659 \pm 0.011$	$0.688 \pm 0.028$
GraphMixer	w/ KEAT	<b><math>0.489 \pm 0.033</math></b>	<b><math>0.458 \pm 0.025</math></b>	<b><math>0.341 \pm 0.002</math></b>	<b><math>0.409 \pm 0.005</math></b>	<b><math>0.675 \pm 0.010</math></b>	<b><math>0.714 \pm 0.024</math></b>
TGN/TGAT	w/o KEAT	$0.435 \pm 0.069$	$0.396 \pm 0.060$	$0.313 \pm 0.012$	$0.349 \pm 0.020$	$0.607 \pm 0.014$	$0.586 \pm 0.037$
TGN/TGAT	w/ KEAT	<b><math>0.515 \pm 0.053</math></b>	<b><math>0.474 \pm 0.031</math></b>	<b><math>0.324 \pm 0.004</math></b>	<b><math>0.380 \pm 0.007</math></b>	<b><math>0.624 \pm 0.012</math></b>	<b><math>0.632 \pm 0.023</math></b>
LeTE	w/o KEAT	$0.431 \pm 0.064$	$0.410 \pm 0.048$	-	-	-	-
LeTE	w/ KEAT	<b><math>0.532 \pm 0.045</math></b>	<b><math>0.483 \pm 0.042</math></b>	-	-	-	-

Table 13: Ablation study on time encoding strategies with and without KEAT across tgbl-wiki, tgbl-review and tgbl-coin datasets. We report validation and test MRR.

Component	GraphMixer	TGN/TGAT	LeTE-Fourier	LeTE-Spline	LeTE-50/50
Memory	172,200	172,400	272,500	262,400	220,250
GAT	67,600	67,800	167,900	157,800	115,650
Link Predictor	20,301	20,301	20,301	20,301	20,301
Time Encoding (TE)	0	200	100,300	90,200	48,050
<b>Total Params</b>	260,101	260,301	360,401	350,301	308,151
<b>% More Params</b>	-0.08%	—	+38.46%	+34.58%	+18.38%

Table 14: Trainable parameters comparison across different time encoding strategies using the TGN backbone for task of link prediction. TGN has three components: memory, GAT, and link predictor, and time encoding (TE) is shared between memory and GAT. LeTE variants differ in how 100-dimensional time encodings are split between Fourier and Spline modeling. Total params = Memory + GAT + Link Predictor – Time Encodings, as time encoder is shared.

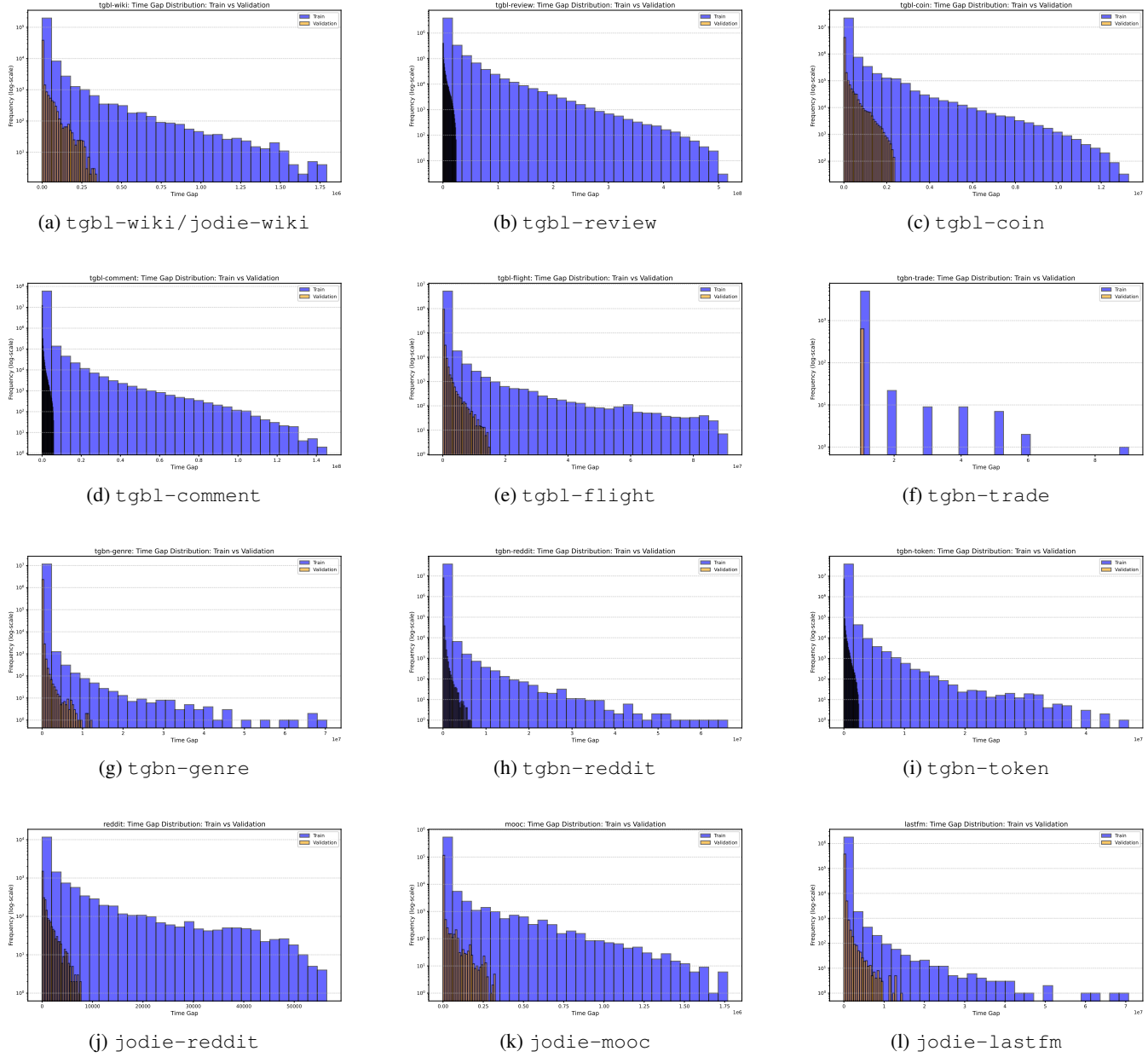


Figure 9: Inter-arrival time distributions  $p(\Delta t)$  for 12 temporal graph datasets. Each subplot shows the distribution of time gaps  $\Delta t$  between consecutive node-level interactions, computed separately for training and validation sets. Noticeable shifts in  $p(\Delta t)$  across these splits indicate temporal distribution drift, which can impact model generalization and motivates the use of kernel-based temporal modulation.

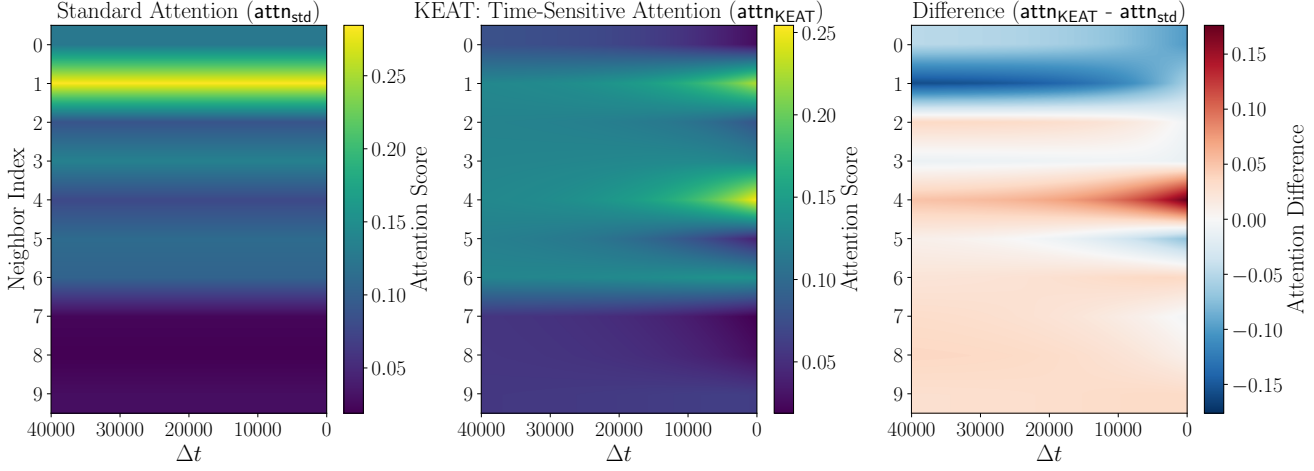


Figure 10: Reproduced temporal attention visualization on  $\text{tgb1-wiki}$  to support interpretability analysis in Appendix G. The figure shows attention weights over ten neighbors across relative time  $\Delta t$ . (Left) Standard attention exhibits **semantic attention blurring**, assigning nearly uniform weights regardless of temporal distance. (Middle) KEAT introduces time-sensitive edge modulation, assigning higher weights to recent and contextually relevant neighbors. (Right) The difference heatmap illustrates how KEAT provides sharper and temporally aware focus. This figure complements the interpretability discussion by showing how attention evolves with edge timing. Figure 11 shows individual neighbor-wise attentions.

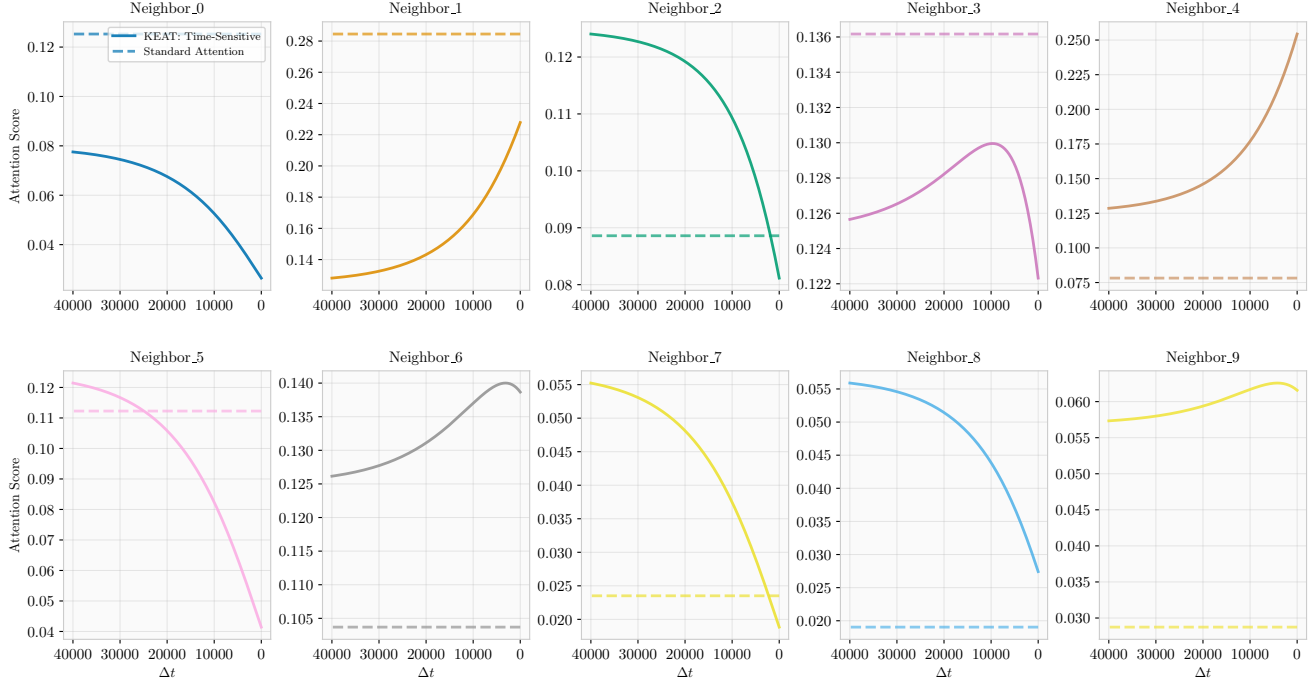


Figure 11: Per-neighbor attention dynamics on  $\text{tgb1-wiki}$  under time-invariant and time-sensitive settings. Each subplot shows attention weights assigned to a specific neighbor across relative time  $\Delta t$ . Lesser value of  $\Delta t$  indicates recent interaction. The two curves represent standard attention and KEAT-modulated (time-sensitive) attention. Standard attention looks time-invariant. KEAT dynamically adjusts attention over time, revealing sharper and more context-aware focus compared to the flatter, temporally agnostic patterns of standard attention.

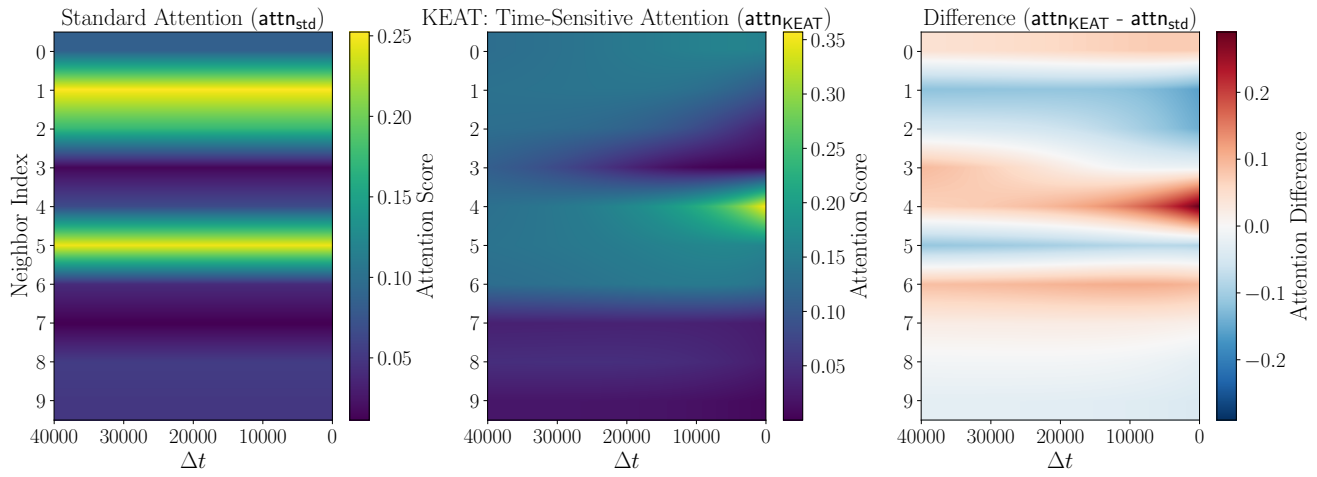


Figure 12: Example 2: Attention visualization,  $\text{tgb1-wiki}$ .

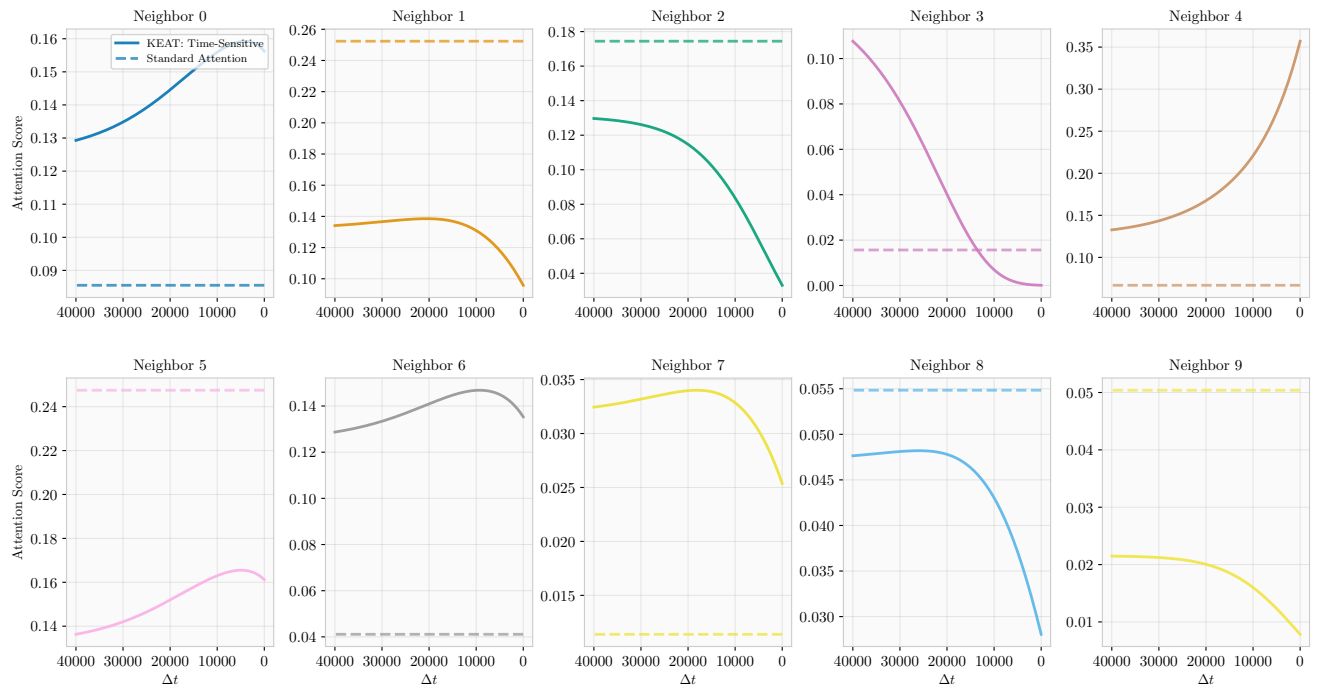


Figure 13: Example 2: Per-neighbor attention visualization,  $\text{tgb1-wiki}$ .

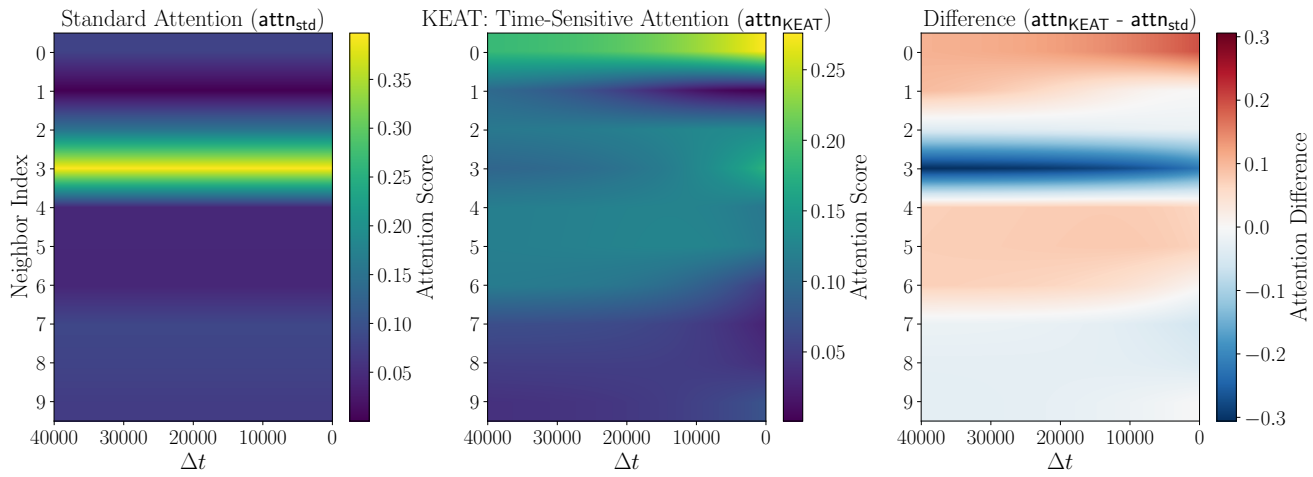


Figure 14: Example 3: Attention visualization,  $\text{tgb1-wiki}$ .

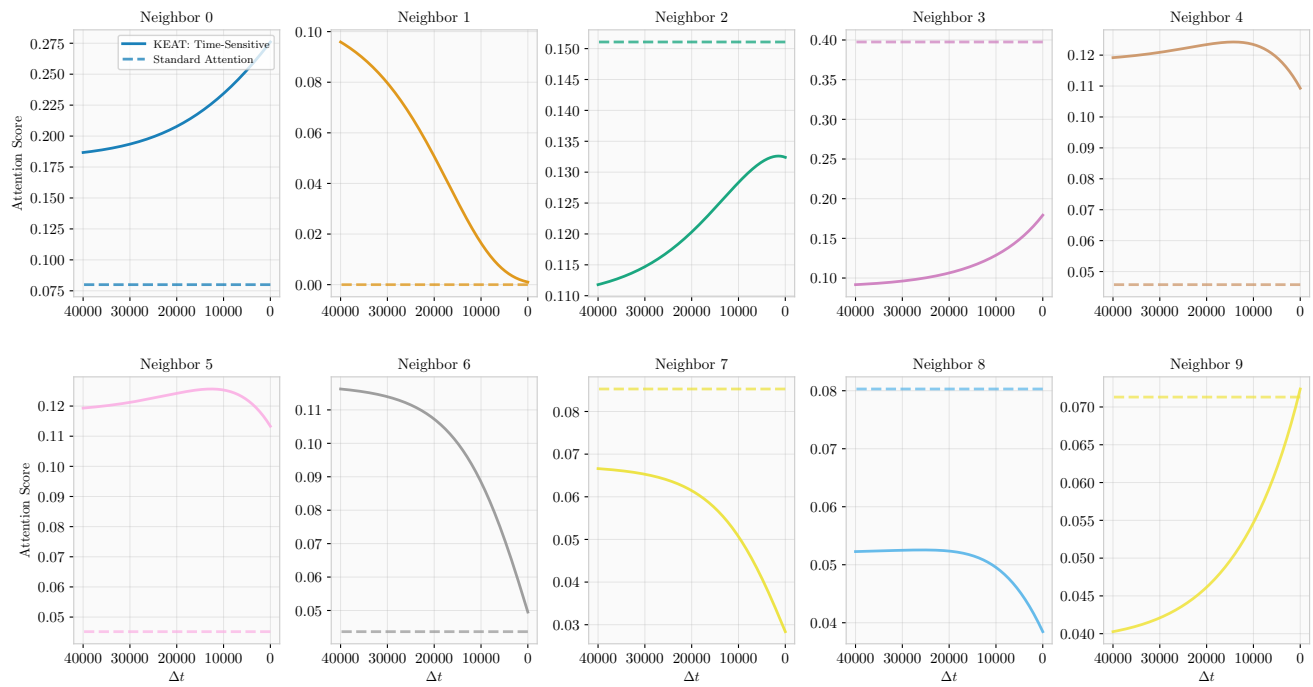


Figure 15: Example 3: Per-neighbor attention visualization,  $\text{tgb1-wiki}$ .